Physical characteristics of kimberlite and basaltic intraplate volcanism, and implications of a biased kimberlite record

Richard J. Brown[1] and Greg A. Valentine[2]

[1]Department of Earth Sciences, Durham University, Durham, DH1 3LE, UK
email: Richard.brown3@durham.ac.uk
[2]Department of Geology, 411 Cooke Hall, University at Buffalo, Buffalo, NY14260 USA
email: gav4@buffalo.edu

Abstract

Bias in the record of kimberlite volcanism is assessed by using newly acquired size data on >900 kimberlite bodies from 12 kimberlite fields eroded to depths of between 0–>1200 m, and by a comparison with intraplate monogenetic basaltic volcanic fields. Eroded kimberlite fields are composed of pipes (or diatremes) and dikes and within any one kimberlite field, regardless of erosion level, kimberlite bodies vary in area at the Earth's surface over 2–3 orders of magnitude. Typically 60–70% of the bodies are <10% the area of the largest pipe in the field. The maximum size of a kimberlite pipe found in a field shows a relationship with estimated erosion levels suggesting that the erosion level of a region could be used to predict the maximum potential size of a pipe where it intersects the surface. The data indicate that the selective removal of surface volcanic structures and deposits by erosion has distorted the geological record of kimberlite volcanism. Selective mining of preferentially large, diamondiferous kimberlite pipes and underreporting of small kimberlite pipes and dikes adds further bias. A comparison of kimberlite volcanic fields with intraplate monogenetic basaltic volcanic fields indicates that both types of volcanism overlap in terms of field size, volcano number and size, and typical erupted volumes. Eroded monogenetic basaltic fields comprise dikes that fed effusive and weakly explosive surface eruptions, and diatremes (pipes) generated during phreatomagmatic eruptions, and are structurally similar to eroded kimberlite fields. Reassessment of published data suggests that kimberlite magmas can erupt in a variety of ways and that most published data, taken from the largest kimberlite pipes, may not be representative of kimberlite volcanism as a whole. This refuels long-standing debates as to whether kimberlite pipes (diatremes) primarily result from phreatomagmatic eruptions (as in basaltic volcanism), or from volatile-driven magmatic eruptions.

Keywords: kimberlite; basalt; monogenetic volcanism; erosion; diatreme; phreatomagmatism

Introduction

All forms of terrestrial volcanism result in the eruption of material onto the Earth's surface and the emplacement of magma and debris in the shallow to deep subsurface. Post-volcanic erosion can expose the subsurface features. The proportions of erupted volume relative to the volume of the shallow subsurface plumbing (or feeder) structure of a monogenetic volcano vary between different eruption styles. Most of the mass of a magmatic (meaning, driven dominantly by expansion of magmatic volatiles) basaltic eruption is emplaced on the Earth's surface as lava or pyroclastic cones; their feeder systems merge downward to narrow dikes within ~200 m below the surface (Keating et al., 2008; Valentine, 2012), and thus have small volumes. In contrast, explosive phreatomagmatic (where magma fragmentation is strongly influenced by explosive magma-water interaction) maar-forming eruptions produce surface tephra deposits, and in the subsurface produce deep, wide diatremes that may have volumes similar to or even larger than the erupted volumes. This results from extensive disruption of country rocks from repeated subterranean explosions, intrusion of magma bodies, and explosion-driven churning and subsidence of material (e.g., Lorenz, 1975; Lorenz and Kurszlaukis, 2007; White and Ross, 2011; Valentine and White, 2012). Landscape erosion can introduce bias into the geological record by removing surface and shallow-level rocks whilst preserving subsurface intrusions, conduits and diatremes. This should apply to kimberlite volcanism, occurring episodically for >1 Ga, in the same manner as it does for all other types of volcanism. Kimberlite eruptions have not been witnessed, surface volcanic deposits and edifices are extremely scarce, and much remains unknown about the behavior of these magmas at the Earth's surface. At the last count, approximately 5000 kimberlite bodies had been documented worldwide (Kjarsgaard, 1996). Most of these are pipes (diatremes filled predominantly with kimberlitic juvenile material and fragmented country rock) or dikes emplaced into stable cratonic crust subject to low rates of erosion (e.g., 10–15 m/Ma, Hanson et al., 2009). The effects of landscape erosion are significant due to the great age of many kimberlites—almost all known kimberlites are Eocene or older. Early models for kimberlite volcanism were strongly influenced by deposits and features of heavily eroded pipes (e.g., Hawthorne, 1975). Current understanding of kimberlite volcanoes is strongly biased because most data have been derived from large subsurface mined kimberlite pipes that have experienced at least several hundred meters of post-emplacement erosion and have lost their upper parts from the geological record (see reviews in Nixon, 1995; Field and Scott Smith, 1999; Field et al., 2008).

In this paper, we ask: how representative is the information gathered from studied kimberlite pipes? What has been the effect of erosion in biasing the record of kimberlite volcanism—what evidence, deposits and structures may have been preferentially removed or emphasized by erosion from kimberlite volcanic fields? We address these questions through a cautious interrogation of size data on >900 kimberlite bodies from 12 kimberlite fields that are thought to have been eroded to various depths, and through comparison with intraplate basaltic volcanic fields which are kimberlites' closest cousins in terms of volume, tectonic setting, and magma composition (note: we include volcanic systems that commonly are, in detail, alkali basaltic or ultramafic in composition). The latter suggests that intraplate basaltic volcanic fields and their eruptions can offer close analogy to some major aspects of kimberlite volcanism, allowing for differences in detail due to magma properties. Analysis of size data from kimberlite fields suggests that the apparent predominance of large pipe structures in many kimberlite fields may result from bias in the geologic record, the selection of mining sites, and underreporting of smaller bodies (dikes and small or shallow volcanic conduits). We argue that the latter are more common than previously recognized, suggesting that large kimberlite pipes represent only a fraction of kimberlite volcanism rather than being representative of it. The apparent dominance of kimberlite pipes in kimberlite fields may have contributed to a misperception that a phreatomagmatic model for the formation of kimberlite pipes (e.g., Lorenz, 1975; Lorenz and Kurszlaukis, 2007; White and Ross, 2011) would seem to require all kimberlite magmas to erupt phreatomagmatically, and in turn, has led researchers to focus on magmatically-driven processes to explain features present in kimberlite pipes (e.g., Hawthorne, 1975; Skinner and Marsh, 2004; Sparks et al., 2006; Wilson and Head, 2007; Cas et al., 2008; Porritt et al., 2008; Brown et al., 2009). The presented data and observations in this paper refuel this debate. The results are of broad interest to those investigating the nature of monogenetic basic and ultrabasic volcanism, intrusive igneous processes in the near-surface, and to geoscientists involved in diamond exploration and mining. The study feeds into investigations of the rates of landscape erosion in continental interiors.

Review of physical geology of kimberlites

Geologic settings, temporal and spatial patterns

Kimberlite pipes, dikes and sills are found on all continents and most are confined to the ancient cratonic regions. They span the early Proterozoic through to the Eocene in age, but worldwide show marked clustering through time. Peaks in kimberlite activity follow major plate re-organizations and coincide with variations in direction and/or in speed in plate motion, and to uplift and erosion

97 relating to episodic tectonic instability and large igneous province (LIP) formation (e.g., Marsh, 1973;
98 Jelsma et al., 2004; Snyder and Lockhart, 2005; Moore et al., 2008; Jelsma et al., 2009).
99 Kimberlites occur in fields (or clusters) that cover hundreds to thousands of square kilometers
100 and contain up to several hundred kimberlite bodies. There is a long-recognized relationship between
101 crustal structure and the distribution of kimberlites and kimberlite fields (Marsh, 1973; Haggerty, 1982,
102 White et al., 1995; Vearncombe and Vearncombe, 2002). Some linear fields parallel geophysical
103 anomalies in the mantle lithosphere (Snyder and Lockhart, 2005) and some are associated with deep,
104 transcontinental crustal fractures or shear zones ("cryptic corridors" of Jelsma et al., 2004). Smaller
105 scale structures control the distribution of kimberlite bodies within fields (Jelsma et al., 2004) and the
106 shapes of pipes (Kurszlaukis and Barnett, 2003; Lorenz and Kurszlaukis, 2007). Individual pipes may
107 be situated at the intersection of major fractures or faults (Dawson 1970; Kurszlaukis and Barnett,
108 2003).
109
110 *Dikes*
111 There are few detailed studies of kimberlite dikes and sills (Dawson and Hawthorne, 1973;
112 Gurney and Kirkley, 1996; Basson and Viola, 2003; Brown et al., 2007; Kavanagh and Sparks, 2011;
113 Gernon et al., 2012; White et al., 2012). Kimberlite dikes occur in regional swarms (Nixon, 1973;
114 Kresten and Dempster, 1973). They are commonly exposed at the same level as large kimberlite pipes
115 in many fields (e.g., Moss, et al., 2009) and occur as late-stage intrusions within pipes (Kurszlaukis and
116 Barnett, 2003). All kimberlite pipes are rooted in dikes. Kimberlite dikes are between 0.03–8 m wide
117 with mean dike thicknesses of ~0.5 m (e.g., Nixon, 1973; Rombouts, 1987; Kavanagh and Sparks,
118 2011). Dikes can form en echelon segments (Basson and Viola, 2003) and are continuous over
119 distances of up to 0.5–10 km, but are probably much longer at depth (Snyder and Lockhart, 2005). We
120 suspect that kimberlite dikes and sills are under-reported within most kimberlite fields due to their poor
121 exposure, small size and mostly poor economic potential, even though they adjacent to most mined
122 kimberlite pipes. It is interesting that numerous kimberlite dikes have been documented in well-
123 exposed regions (e.g., Lesotho; Nixon, 1973).
124
125 *Kimberlite pipes*
126 Kimberlites pipes are downward-tapering volcanic conduits with upper diameters that may
127 exceed 500 m. They can reach >2 km deep and have volumes of 10^6–10^8 m^3 (e.g., Clement, 1982;
128 Nixon, 1995; Field and Scott Smith, 1999; Field et al., 2008). The walls of kimberlite pipes generally
129 dip inward at steep angles (~80–85º) but may dip at shallower angles, and be vertical or slightly

outward-dipping over scales of tens to hundreds of meters. Dip angles in the near surface may be shallower due to cutting through weak sediment layers and through neighboring pipes (e.g., Field et al., 1997; Kurszlaukis et al., 2009). In cross-section (map view) they are roughly circular to ellipsoidal and may become more irregularly shaped downward. The orientation of joints and faults in the country rock and the regional stress field can influence the shape of pipes (e.g., Barnett, 2008). Lower parts of kimberlite pipes (root zones, e.g., Clement, 1982) transition into dikes.

Kimberlite pipes are filled with a variety of rocks and no two kimberlite pipes are exactly alike (see Field and Scott Smith, 1999; Sparks et al., 2006; Kjarsgaard, 2007). Most pipes contain rocks composed of juvenile pyroclasts, phenocrysts, mantle debris and crustal rocks, the latter derived predominantly from host rocks that occupied the volume of the pipe prior to eruption. Volcaniclastic rocks within kimberlite pipes can be massive or layered. Layered volcaniclastic kimberlite lithologies include pyroclastic and sedimentary rocks that exhibit bedding and stratification on different scales and defined by variations in grainsize and/or composition. Massive volcaniclastic rocks commonly show evidence for gas fluidization including restricted grainsize distributions, gas escape pipes, and homogenous mixing of lithic clast types (Walters et al., 2006; Gernon et al., 2008), although the role of wholesale (versus local, meters to tens of meters scale) fluidization of kimberlite pipes is contentious (e.g., White and Ross, 2011). Matrix- to clast-supported marginal wall rock breccias occur at many levels (e.g., Barnett, 2004; Brown et al., 2009). Dikes, sills, bulbous intrusive bodies, lavas and lava lakes and welded pyroclastic rocks have also been recognized in some pipes (e.g., Brown et al., 2008a). Rock units and lithofacies within kimberlite pipes are commonly arranged in pseudo-concentric patterns, forming complex structures that might indicate alternating erosion and filling phases (see Kjarsgaard, 2007; Field et al., 2008 and references therein; Brown et al., 2009). Kimberlite pipes and their contained deposits share many structural and geological characteristics with diatremes beneath maar volcanoes (e.g., Lorenz, 1975; Lorenz and Kurszlaukis, 2007; White and Ross, 2011).

Sizes of kimberlite volcanoes and their plumbing systems

Much of the data on kimberlite fields is not in the public domain but we have obtained a unique dataset on the sizes (plan view area) of 912 kimberlite bodies from 12 kimberlite fields in seven countries (Table 1). The data represent geophysical anomalies detected mostly during aerial magnetic surveys and field campaigns. The reported kimberlite bodies are variably buried beneath glacial till, desert sand or soil, or are exposed to varying degrees at the Earth's surface. Cross-section (map view) shape data for the kimberlite bodies is not available. The size data are reported in square meters and as diameters derived from the square root of the area. Caution is needed in interpreting the data because

the size of a geophysical anomaly can be dependent on lithology (magnetic vs. non-magnetic lithologies) and because not all anomalies have been confirmed by drilling (or the data are not available). The sizes of geophysical anomalies in shallowly-eroded kimberlite fields (Table 1) need to take into account crater flaring and coalescence with neighboring kimberlites. Dikes are less likely to be detected by geophysical surveys especially when the country rock has a strong magnetic signature. The amount of erosion is difficult to assess and poorly quantified: erosion estimates have been derived from several different qualitative lines of evidence (e.g., regional stratigraphic surveys, geological mapping and the lithic inclusions contained within kimberlite pipes; Hanson et al., 2009). Below we illustrate the main features of kimberlite fields that are thought to have experienced between 0–1250 m erosion. We consider that the estimates of erosion may well have errors of ±200 m. Nevertheless, we consider that general trends drawn out of the dataset, which represents 15–20% of known kimberlite bodies worldwide, are representative enough of kimberlite volcanism to make some valid observations, tentative interpretations and draw some preliminary conclusions. This is supported by the similarity in the size distributions of different kimberlite fields.

Little eroded kimberlite fields

The only known examples of exposed kimberlite edifices are the three Holocene Igwisi Hills volcanoes (IHV), Tanzania (Fig. 1; Dawson, 1994; Brown et al., 2012). These are small volcanoes with erupted volumes of >0.001 km^3 (Fig. 1). The NE volcano resembles a small maar volcano with a 200 m diameter crater at or near the pre-eruptive surface. A 500 m-long lava flow extends away from the NE of the volcano. The central volcano has a partial tephra cone built up on the NW side of a <100 m diameter crater filled with a lava coulee (Brown et al., 2012). The SW volcano is a small pyroclastic cone, with a perched crater, <180×100 m in diameter. Crater surface areas at the pre-eruptive surface range from $<7\times10^3$ to 3×10^4 m^2. The central and SW volcanoes share similarities with basaltic scoria cones. There is little evidence for substantial excavation of deep conduits beneath the volcanoes and Brown et al. (2012) concluded that the conduits beneath the central and SW volcanoes were probably similar in dimensions to those beneath basaltic scoria cones (c.f., Keating et al., 2008; Valentine, 2012).

The >69 Cretaceous Fort à la Corne kimberlites (Fig. 2), Canada, are presently buried under thick glacial till and comprise pyroclastic rocks and reworked volcaniclastic rocks emplaced in a coastal or submarine environment (e.g., Leckie et al., 1997; Berryman et al., 2004; Pittari et al., 2008). They have been interpreted as either shallow, wide craters filled with pyroclastic rocks (Berryman et al., 2004), or positive relief tephra cones and tuff rings (Leckie et al., 1997; Zonneveld et al., 2004;

Kjarsgaard, 2007; Harvey et al., 2009), or some combination of the two (Pittari et al. 2008; Lefebvre and Kurszlaukis, 2008). Conduits have been drilled to depths of 700 m. Seismic reflection surveys of the kimberlite body 169 outlines a cone 50–100 m high and >1 km in diameter (e.g., Kjarsgaard, 2007). The near-shore setting has led many authors to infer that the eruptions were in part phreatomagmatic (Lefebvre and Kurszlaukis, 2008; Pittari et al., 2008; Kjarsgaard et al., 2009). Substantial kimberlite pipes have not been located beneath the Fort à la Corne kimberlite volcanoes. This may indicate similarities to basaltic tuff rings and tuff cones where phreatomagmatic explosions were very shallow or/and dominated by surface water rather than groundwater (see White and Ross, 2011).

The Cretaceous Alto Cuilo kimberlite field, Angola, comprises >200 kimberlites buried under Kalahari sand (Pettit, 2009; Table 1). The kimberlites erupted through Karoo sediments and have been imaged primarily by airborne magnetic surveys. Kimberlite craters, and in some cases, extra crater lavas are unusually well preserved (Eley et al., 2008). Shallow geophysical data suggest that some large craters appear to flare upwards. Geological data are sparse on each target, but some general statements can be made about the field, based on the size data. Approximately 60% of the kimberlites are <400 m in diameter (1.2×10^5 m^2), and approximately 30% are <250 m in diameter (1.9×10^5 m^2, Fig. 3). There is limited information on the nature of the preserved volcanoes: some may represent eroded craters, while others may still have surface parts of cones preserved. Pettit (2009) considered that they are comparable to the Fort à la Corne kimberlite volcanoes (Table 1).

Other examples of kimberlite volcanoes include the Meso-Neoproterozoic Tokapal kimberlite, India (Mainkar et al., 2004)—a 2 km wide, 70 m thick buried and eroded tuff ring.

Shallowly eroded kimberlite fields

The 85 kimberlites of the Cretaceous Orapa kimberlite field, Botswana, are considered to have experienced <200 m erosion since emplacement (Table 1; Field et al., 1997; Gernon et al., 2009a, b). The largest kimberlite pipe (A/K1 South) has a flared crater that has cut into the neighboring pipe (A/K1 North). 98% of the kimberlites are <400 m in diameter (1.2×10^5 m^2); approximately 47% are <110 m (1.1×10^4 m^2) in diameter and 25% are <50 m in diameter (2×10^3 m^2; Fig. 3). Dikes have been uncovered by mining operations around the large kimberlite pipes although data are sparse.

Cretaceous kimberlites in Northern Lesotho have been subject to ~300 m of erosion (Hanson et al., 2009) and are exposed over an area 10×100 km (Dempster and Tucker, 1973; Kresten and Dempster, 1973; Nixon, 1973; Jelsma et al., 2009). Due to the mountainous terrain and thin patchy overburden numerous kimberlite dikes are exposed (Fig. 4). Nixon (1973) reports a dike swarm, trending 300°, with >220 individual dike segments, 21 blows ~8–40 m wide (or ‘buds’ sensu Delaney

and Pollard,1981, thicker sections along dikes that may contain breccia), and 17 pipes between 70–500 m in diameter (1.5×10^4–8×10^5 m^2). Pipes contain volcaniclastic rocks. Individual dike segments are 0.1–7 m wide and 50% are continuous over <50 m, although this is controlled largely by exposure. Some 13% can be traced for over 1 km. The longest extends for >9 km.

Moderately eroded kimberlite fields

The 159 Upper Cretaceous to Paleogene Ekati kimberlites, Canada (Table 1) are thought to have experienced several hundred meters erosion (<500 m; Nowicki et al., 2004). The largest pipe has a diameter of 450 meters. Approximately 60% are <100 m in diameter; 10% are <60 m in diameter. Dikes are common adjacent to the pipes (Nowicki et al., 2004).

The Cambrian Venetia kimberlite field, South Africa, is considered to have been eroded to depths of ~500 m and comprises >15 pipes and dikes (Table 1, Kurszlaukis and Barnett, 2003). The erosion level has been estimated from the presence of Karoo sedimentary rocks in the pipes which have been eroded from the region. The largest pipe, K1, is irregular, elongate, and is 650×250 m in diameter (1.2×10^5 m^2). Eleven of the pipes are <90 m in diameter (<6×10^4 m^2). Some kimberlite bodies are dikes (e.g., K8 kimberlite, Kurszlaukis and Barnett, 2003) and late-stage dikes are present within the large pipes and around them.

Deeply eroded kimberlite fields

Two groups of kimberlites outcrop in the Kimberley area, South Africa. A younger group emplaced around 111–97 Ma, is thought to have experienced ~850 m of erosion (Hanson et al., 2009). This group comprises 68 kimberlite bodies, the largest of which is 400 m in diameter (1.3×10^5 m^2, Fig. 3); 42% are <110 m in diameter and 25% are <60 m in diameter.

The older group (119–114 Ma) comprises 134 kimberlites that have experienced ~1250 m of erosion (Hanson et al., 2009). The largest pipe is 270 m in diameter (5.5×10^4 m^2). 80% are <100 m in diameter and 35% are less than 40 m in diameter (Fig. 3).

General trends

These newly acquired data from kimberlite fields exposed at various paleo-depths allow us to examine the subsurface plumbing systems of kimberlite fields. The eroded kimberlite fields are composed of pipes and dikes, but the data do not allow distinction between dikes and small pipes because shape data are lacking. Within any one kimberlite field, regardless of erosion level, kimberlite bodies vary in area over 2–3 orders of magnitude (Fig. 3)—typically 60–70% of the bodies are <10%

of the area of the largest pipe in the field. Those kimberlite fields inferred to have undergone a greater degree of erosion are composed of collectively smaller kimberlite bodies than the less-eroded fields (Fig. 3). This can be illustrated by plotting the area of the largest kimberlite pipe within a field against the estimated amount of erosion that each field has experienced (Fig. 5). The largest kimberlite bodies (<1500 m in diameter) are found in shallowly-eroded fields and may represent flared surface craters or coalesced neighboring pipes. Flaring of volcanic conduits in the near-surface is common (e.g., Keating et al., 2008; Ross et al., 2011; White and Ross, 2011) and can reflect: (1) more energetic explosions that disrupt more country rock at shallow depths compared to deeper explosions (Valentine and White, 2012); (2) syn-eruptive collapse into the conduit of weak or poorly consolidated host rocks or neighboring kimberlite pipes; and (3) post-eruption collapse of crater walls (e.g., Pirrung et al., 2008). At 200–300 m erosion depths, non-flared kimberlite pipes have diameters up to ~500 m (8×10^4 m^2), while those with flared craters (Orapa and Yubileina) are up to 900 m in diameter (6×10^4 m^2). The diameters of the non-flared portions of the Orapa and Yubileina kimberlite pipes (~500 m depth) compare well with the maximum size of other kimberlite pipes at inferred equivalent depths (Fig. 5). At 500–800 m of inferred erosion levels (e.g., Venetia and Kimberley Group 1 fields, Table 1) the largest kimberlites are 300–400 m in diameter (8×10^4–1.2×10^5 m^2;), and at >1200 m erosion depths (Kimberley Group 2 field, Table 1) the largest kimberlite is only 260 m in diameter (5.5×10^4 m^2). Acknowledging the uncertainties over paleo-depths from surface, the rate of decrease of maximum pipe sizes for erosion, from 1250 m (shallow) to 200 m (deep), is broadly consistent with pipe walls dipping inward at the typical observed slope angles of ~82–85° (equivalent to a 30 m decrease in diameter for every 100 m loss in height, Fig. 5).

Review of physical geology of intraplate basaltic fields and their plumbing

Geologic settings, temporal patterns

Basaltic volcanic fields occur in nearly all tectonic settings, including hot spot (e.g., Snake River Plain, U.S.A.; Kuntz et al., 1986), subduction zone (e.g., Michoacán-Guanajuato, México; Hasenaka and Carmichael, 1985), and back-arc (e.g., Ojikajima, Japan; Sudo et al., 1998). Here we focus on intraplate occurrences, which offer a closer analogy to the settings of most kimberlites. Intraplate basaltic fields occur far away from active plate margins on all continents and on the sea floor away from spreading centers (Hirano et al., 2006), and are dominated by monogenetic volcanoes. Fields typically are active for several millions of years: within many volcanic fields there are very young, well preserved volcanoes in proximity to eroded volcanoes, including those whose plumbing is

exposed, providing excellent opportunities to relate subsurface structure to eruptive processes and landforms (e.g., Hopi Buttes; White, 1991).

Most intraplate volcanic fields have alkali basalt affinities and are thought to represent low degrees of partial melting at depths of ~50–100 km. Some magmas appear to be sourced in lithospheric mantle, particularly early in a volcanic field's lifetime, while others have OIB compositions and some are ultramafic (e.g., minette, nephelenite, and other compositions). Mantle-derived xenoliths are common, but not ubiquitous. Many authors assume that this implies rapid ascent of the host magmas, but effusively-erupted lavas, as well as explosively erupted juvenile-rich pyroclastic deposits, contain mantle xenoliths and, therefore, their presence cannot imply explosive decompression from mantle depth as is sometimes inferred (e.g., McGetchin and Ullrich, 1973). Crustal xenoliths also occur in intraplate basalts but their abundance is strongly dependent upon whether eruptions are phreatomagmatic or magmatic (e.g., Valentine and Groves, 1996; Valentine, 2012).

Spatial occurrences

Like kimberlites, volcanoes in basaltic fields occur in a range of patterns from isolated to randomly distributed to fielded and aligned. Fields with tens or more volcanoes typically show some sort of fielding; a well-studied example is the Springerville field in Arizona, U.S.A. (Condit and Connor, 1996). The volcanoes in fields typically form over a span of time such that volcanic constructs overlap and bury each other where the vent density is very high, blurring the distinction between monogenetic and polygenetic activity. Conway et al. (1997) show how vent locations within fields can be closely associated with pre-existing, major crustal faults. Whether this association is simply a reflection of dikes preferentially ascending through weak zones in the crust, as is often assumed, or whether there is a link between crustal structure and deeper melt collection processes, is a question that remains open. Mazzarini and D'Orazio (2003) and Lesti et al. (2008) describe evidence of alignments and fields over ranges of length scales from hundreds of meters to tens of kilometers, and describe how these alignments relate to pre-existing crustal structure and to the thickness and mechanical properties of the lithosphere. At a local level, individual volcanoes, whether scattered or aligned with others, often occur along pre-existing faults (e.g., Hirano et al., 2006; Valentine and Krogh, 2006) that may not be oriented perpendicular to the least principal stress that normally controls dike orientation, although there are only limited conditions under which this process of "dike capture" can occur (Connor and Conway, 2000; Gaffney et al., 2007). Such relationships between pre-existing structure and vent location can be most pronounced in volcanic fields that have relatively low long-term magma fluxes (tectonically controlled fields; Valentine and Perry, 2007).

Dimensions of intraplate basaltic volcanoes and their plumbing structures

Scoria cones

Scoria cones have typical basal diameters of ~400 m up to ~2.5 km (median value ~900 m; Wood, 1980), with summit craters that are typically ~40% as wide as the cone base (Wood, 1980). For our purposes, the measurement that is comparable to maar crater size is probably not the summit crater but the conduit or feeder dike width at the pre-eruptive surface, which is discussed below.

Keating et al. (2008) provide the only quantitative data that we are aware of on the shallow plumbing of small volume, intraplate basaltic volcanoes dominated by magmatic eruptions (e.g., Strombolian, violent Strombolian, and Hawaiian). In the best constrained exposed plumbing systems that they described, vent structures are several tens of meters up to ~200 m wide at the paleo-surface, and the walls of the plumbing converge rapidly downward toward the feeder dike. The vent structures are much smaller than the typical footprint of the scoria cones that accumulate above them. The depth over which the vent structure transitions from its maximum width at the surface, to the feeder dike below, is also typically 10s of meters (in other words, the depth of the vent structure is similar to its diameter at the pre-eruptive surface, implying that vent complex margins dip inward ~60–70°).The feeder dikes observed by Keating et al. (2008) typically range between 1–10 m wide to depths of ~250 m, and it is likely that they narrow below that depth because of increasingly limited interaction with the free surface. Indirect data based upon wall rock lithic contents from magmatic eruption products (Valentine and Groves, 1996; Valentine et al., 2007; Valentine, 2012) are consistent with volcano plumbing with widths on the order of ~tens of meters and less at depths <200 m. This can be complicated by widening produced by minor phreatomagmatic phases during an otherwise magmatic-dominated eruption. For example the Tolbachik scoria cone eruptions had brief phreatomagmatic phases that might have widened their plumbing by ~8–48 m at depths of >500 m (Doubik and Hill, 1999), based upon the volume of erupted xenolith material, and assuming a 1600 m deep cylindrical conduit. It seems also reasonable that below a few hundred meters depth the plumbing geometry was that of a dike: the same xenolith volume could have been produced by only widening the dike by a few decimeters. To summarize, it appears that in most cases, the plumbing of monogenetic volcanoes dominated by magmatic eruptions is represented by relatively thin dikes at depths greater than ~200 m. Note that recent data (Geshi et al., 2010) suggest that the vent structures for small-volume basaltic eruptions can be much smaller, perhaps only a few meters wide at the pre-eruptive surface, although these data were measured on basaltic vents on a larger stratovolcano rather than an intraplate setting.

Maars

Surprisingly few data compilations of maar crater sizes are available. Maar/tuff ring crater diameters for the examples in Table 2 range from 100-2000 m. Taddeucci et al. (2010) report maar diameters of 623–2536 m in the Alban Hills (Italy). Beget et al. (1996) document maars with diameters between 4000–8000 m, but these appear to be compound maars formed by the coalescence of multiple craters. Cas and Wright (1987) provide a histogram of crater diameters based upon data from 116 maars. The distribution ranges from 200–3200 m with most craters between 400–1400 m and a mode of ~800 m. Unfortunately, the source data were never published, so it is not possible to reproduce the data or to understand the details of where and how the measurements were taken. Ross et al. (2011) provide crater depths and diameters for Quaternary maars, showing that the diameters range from ~100–1700 m, with most falling between 400–1200 m. It seems that ~400–1200 m is a reasonable representative diameter range for monogenetic maar and tuff ring craters.

White and Ross (2011) review diatremes formed beneath phreatomagmatic maar volcanoes, and compare them with kimberlite pipes. They conclude that the two types of features are similar in most of their physical characteristics. The phreatomagmatic diatreme literature includes some qualitative descriptions and diagrams of the vertical extent of diatremes (Lorenz, 1986; White, 1991; Martin and Németh, 2005; Auer et al., 2007; Lorenz and Kurszlaukis, 2007; McClintock et al., 2008) that give a sense of the vertical dimensions, but without any direct measurements due to the nature of exposures. Indirect data from wall rock lithic abundances support the general conclusion that diatremes for phreatomagmatic basaltic volcanoes extend 100s of meters to ~ 2 km depth (Lorenz, 1979; Valentine and Groves, 1996; Valentine, 2012), implying typical diatreme-country rock contacts dipping steeply inward from the surface crater diameters described above (White and Ross, 2011; also supported by limited geophysical data such as in Matthes et al., 2010). Diatremes can be less deep and with gentler dipping walls if host material is unconsolidated sediment and magma-water interaction is near or at the Earth's surface, (e.g., Ross et al., 2011; Blaikie et al., 2012). Most of the country rock disrupted by phreatomagmatic explosions remains within the diatreme, while only relatively shallow-seated explosions actually eject material out of the maar crater (strictly speaking, "shallow" is a relative term that depends upon explosion energy and should be referred to as "scaled depth;" e.g., Goto et al., 2001). Deep-seated country rock lithic clasts are mixed upward within the diatreme by subterranean explosions that may not directly erupt (debris jets, Ross and White, 2006; Ross et al., 2008a,b), and the lithic clasts are subsequently ejected onto the surface by shallow explosions (Valentine and White, 2012), rather than being directly ejected from deep explosions as was suggested by Lorenz (1986).

Conversely, shallow-derived material, including tephra deposited on maar crater floors and material shed from collapsing crater walls, can be mixed downward by subsidence.

Relative proportions of phreatomagmatic vs. magmatic volcano types in intraplate basaltic fields

Intraplate, monogenetic basaltic volcanic fields are composed of varying combinations of scoria cones and their attendant lava fields, maars, small lava shields, and tuff rings and cones (the latter usually found where basalt erupted through standing surface water). Scoria cones, maars, and tuff rings are the most common vent-related landforms. Despite their abundance on the planet, there are surprisingly few well-documented data on the relative proportions of these dominant landforms. Table 2 compiles data from fifteen volcanic fields for which we were able to find specific mention of the relative proportions of vent-related landforms. Eight of the volcanic fields contain 0–10% maars or tuff rings, the remaining vent-related landforms being dominated by scoria cones. It is worth noting that many of these are in arid or semi-arid climatic settings. The remaining four contain ~20–30% maars and tuff rings and are characterized by wetter climates, with the partially marine Auckland Volcanic Field potentially as high as 70% maars/tuff rings. The "footprints" of scoria cones are similar to the sizes of maar/tuff ring craters (see below), thus it is important to keep in mind that these proportions might underestimate the number of maars/tuff rings to some degree, because some volcanoes might have opening or early phreatomagmatic phases that later transition to magmatic activity which buries the early features in scoria, spatter, and/or lava (e.g., Lorenz and Büchel, 1980; White, 1991). The opposite can occur as well, where an eruption begins with scoria cone building that is later partly or wholly destroyed by phreatomagmatic maar forming activity (Gutmann, 2002). In two of the example volcanic fields in Table 2 (Southwest Nevada Volcanic Field, and Lunar Crater Volcanic Field), old and eroded vents, where early phreatomagmatic phases should crop out, do not indicate a significant number of "hidden" maars/tuff rings. Both of these volcanic fields reside in an arid region, and it is unclear whether this observation can be extended to volcanic fields in wetter settings.

Dikes

The magmas that feed intraplate monogenetic volcanoes ascend from their mantle sources via dikes, as do kimberlite magmas. The detailed structures within dikes associated with these volcanoes can show evidence for multiple pulses of magma (e.g., nested quenched margins and vesicle bands). This is especially true in the very shallow crust and where dikes extend within the volcanic constructs; Hintz and Valentine (2012) suggest that such pulsing reflects both variations in magma supply rate from depth, and shallow processes such as gas slugs ascending through volcanic plumbing (and

ultimately causing Strombolian bursts at the surface) and temporary vent blockage. Other dikes appear to have been emplaced in one event that had little temporal variation.

The dimensions of intraplate basaltic dikes are similar to those described for kimberlites. At shallow depths (~200 m or less), dikes can be several meters wide and locally wider where conduit structures have formed along them (Keating et al., 2008). Dike lengths at these depths range from hundreds of meters to a few kilometers (Valentine and Perry, 2006; Valentine and Keating, 2007). Sills can form at these shallow depths, especially along country rock bedding planes or where there are contrasts in rock properties (Kavanagh et al., 2006; Valentine and Krogh, 2006). Dikes exposed at deeper emplacement depths are notably thinner; Delaney and Gardner (1997) report a median dike width of 1.1 m (Utah, USA), which is inferred to be the feeder system of a deeply eroded (~400–2000 m below paleo-surface) basaltic volcanic field. The same area has a median dike length of 1090 m, although in detail each dike crops out in many shorter segments (Delaney and Gardner, 1997).

Effects of landscape erosion on preservation of volcanic plumbing

We now explore how a typical basaltic volcanic field might be represented in the geologic record of an area that undergoes progressive landscape erosion. Consider a volcanic field that, when active and un-eroded, has 90% scoria cones and 10% maars/tuff rings (Fig. 6), a reasonable scenario (Table 2). These proportions are based on a count of vent types. The relative area fractions presented by the two types of vent structures would be approximately equivalent to the proportions based upon a vent-type count in this young field because the footprints of scoria cones are similar in size to those of maars/tuff rings.

As the landscape erodes, pyroclastic deposits left by both magmatic and phreatomagmatic eruptions are removed relatively quickly, within a few Ma. Once the erosion level is generally close to the pre-eruptive surface, a geologic map would show areal proportions of volcanic features of ~50% scoria cone vent structures, and ~50% upper diatremes associated with maars and tuff rings. This reflects the difference in the scale of the upper plumbing of the vent types; even though the number of vent types remains the same, the scoria cone plumbing is about a factor of ten smaller (~100 m diameter) than the upper parts of diatremes (equivalent to the maar/tuff ring crater diameters—typically ~1000 m in diameter). When the landscape has been exhumed to ~100–200 m below the pre-eruptive surface, vent structures for most scoria cones will have completely merged into their feeder dikes, while diatremes associated with former maars/tuff rings might still have significant areal extent. Assuming that the feeder dikes average ~2 km in strike length and range between 2–5 m wide, a geologic map of the volcanic field once it has eroded to 300 m depth would have areal proportions of

volcanic (hypabyssal) features of ~80–90% diatreme material and ~10–20% feeder dikes (see Fig. 6). When erosion has stripped 1000 m, these areal proportions would comprise ~50–75% diatreme and ~25–50% feeder dike, because as the diatremes continue to narrow downward the dikes maintain a relatively constant geometry.

This is a hypothetical example showing that even if phreatomagmatic-dominated volcanoes are the minority in a volcanic field, landscape erosion will emphasize their plumbing structures compared to the more dominant magmatic-dominated structures. Other examples with different proportions of maars and scoria cones will have correspondingly different proportions of their respective plumbing features as the landscape erodes. However, it is clear that the differing physical scales of magmatic versus phreatomagmatic shallow plumbing result in an apparent predominance of phreatomagmatic features (diatremes) as a landscape is eroded.

Comparison of kimberlites and intraplate basaltic volcanic fields

Our investigation of kimberlite and basaltic monogenetic fields indicates that they have more in common than they do have differences. The few kimberlite volcanoes that have been described (Igwisi Hills volcanoes and the Fort à la Corne kimberlites) have surface dimensions that overlap with those of small monogenetic basaltic volcanoes (scoria cones, maars, and tuff rings and cones) and the eruptions that formed them were probably of similar magnitude to monogenetic basaltic eruptions. They provide little direct evidence for substantial subsurface diatremes and some may instead sit upon small volcanic conduits that transition into dikes at 200–300 m depth (e.g., Brown et al., 2012). They provide evidence that kimberlite magma can erupt in a variety of ways that are comparable to basaltic volcanism (e.g., explosively, effusively and phreatomagmatically; e.g., Kjarsgaard et al., 2009).

The general subsurface plumbing systems (i.e., dikes versus diatremes) of both kimberlite and basaltic fields are similar, accounting for post-volcanic landscape erosion. We note that most published data on and interpretations of kimberlite volcanism are derived from studies of very large diamond-bearing kimberlite pipes that have been exposed by mining. These are mostly the largest ~5% of the ~900 kimberlite bodies used in this study. Our concern is that this could be equivalent to trying to describe monogenetic basaltic volcanism only from studies of eroded maar volcanoes whose craters exceed 1.5 km in diameter. Many smaller kimberlite bodies in kimberlite fields remain unstudied and comparisons between these and large mined kimberlite pipes are largely unexplored. Mining of many large kimberlite pipes reveals dikes and smaller pipes in the surrounding country rock and where kimberlite fields are well exposed dikes are abundant (e.g., Lesotho; Fig. 4 and Table 1). The ratio of dikes to pipes at different levels within kimberlite fields is not known. We suggest that the apparent

predominance of kimberlite pipes within fields in the geological record is at least partly a result of erosional bias due to removal of small and shallow volcanic structures and of the under reporting of kimberlite dikes due to their low economic importance and difficulty of geophysical detection. We suggest that kimberlite dikes may well be as common in kimberlite fields as they are beneath monogenetic basaltic fields.

The maximum size of a kimberlite pipe in a field appears to show a predictable relationship with erosion depth (at depths >200 m) equivalent to a structure with inward-dipping walls sloping at 80–85° (Fig. 5). Acknowledging uncertainties over erosion depths, this may indicate that: A) it may be reasonable to use these slope angles to extrapolate deeply-eroded pipes upwards to within 100–200 m of the paleo-surface to estimate original dimensions; B) that there may be a maximum size that kimberlite pipes can grow to, probably due to a combination of dynamic (e.g., duration of eruption) and slope stability reasons (e.g., Sparks et al., 2006) and; C) that estimations of the erosion level of a region could be used to predict the maximum potential size of a kimberlite body expected in a newly identified field. By extrapolation, the 24% of kimberlite bodies that are <50 m diameter at <200 m depth in the Orapa field (Fig. 3) would have had surface crater diameters of <110 m (not accounting for any surface flaring) and would be less than 20 m wide at >300 m depth. Similarly, ~40% of kimberlite pipes in the Orapa field would have been <160 m wide at the surface and would be <10 m diameter at 500 m depth. These extrapolated conduit dimensions are approaching the dimensions of those below scoria cones (e.g., Keating et al., 2008) and are comparable to the crater dimensions inferred below Holocene kimberlite scoria cones (Brown et al. 2012). This suggests to us that the Orapa kimberlite field may have contained small volcanoes which had little subsurface expression. In basaltic fields eroded to similar depths, subsurface diatremes typically account for between 0–30% of the feeder structures (the others being dikes; Table 2). Should a similar ratio hold true for kimberlites then the Orapa kimberlite field may have originally contained many more volcanoes, now lost through erosion. Thus some kimberlite fields may have had >400 volcanoes and, for example, if each eruption emitted 0.001–0.01 km^3 of magma (typical volumes for monogenetic eruptions), then 0.4–40 km^3 of kimberlite magma could have made its way to the surface over the lifetime of a large kimberlite field.

That numerous kimberlite dikes are found at shallow levels in the crust (e.g., <300 m, Fig. 4) in some places indicates that kimberlite magma can rise to the near-surface without disintegrating into explosive flows that carve out wide and deep vents (pipes). This suggests that kimberlite magma may be commonly capable of feeding weakly explosive or effusive eruptions (e.g., Igwisi Hills volcanoes; Brown et al., 2012) in a manner typical of basaltic magmas. By analogy with intraplate, monogenetic basaltic volcanoes, the volume fluxes of these eruptions probably are <c. 10 m^3/s. This begs the

question, why would some rising batches of kimberlite magma instead create deep pipes? In basaltic fields similar structures (diatremes) are generated by explosive interaction of magma with groundwater. A phreatomagmatic origin for kimberlite pipes has been proposed and elaborated (Lorenz, 1975; Lorenz and Kurszlaukis, 2007; White and Ross, 2011), but is not universally accepted, despite many similarities between diatremes constructed beneath maar volcanoes and kimberlite pipes. This is due in part to the unusual characteristics of kimberlite melts (e.g., very low silica contents, high CO_2 and H_2O contents, inferred low magmatic viscosities and high degrees of mantle and crustal contamination; Mitchell 1986; Sparks et al. 2006), and resulting uncertainties over how they behave in the near-surface. High volatile contents are thought to enable kimberlite magmas to rise rapidly (Russell et al., 2012) and allow kimberlite magmas to erupt explosively and excavate wide, deep pipes (Sparks et al., 2006; Wilson and Head, 2007; Cas et al., 2008). Additionally, paleomagnetic studies of pyroclastic deposits within some kimberlite pipes indicate high (magmatic) emplacement temperatures (Fontana et al., 2011). An in-depth exploration of the behavior of volatiles in kimberlite melts is beyond the scope of this paper, but variations in the initial volatile loads or in the degassing history of successive batches of rising kimberlite magma could explain the variation in near-surface behavior, with volatile-rich batches erupting explosively and creating kimberlite pipes. However, a problem remains—if (volatile-poor) kimberlite magma can rise in dikes to the near-surface without excavating pipes, then what is to stop that magma interacting with groundwater to produce diatremes in a similar manner to basaltic magmas in near-surface dikes? In this case how might you distinguish a pipe created by a magmatic eruption from one created by a phreatomagmatic eruption? Some kimberlite pipes contain features indicative of magma-water interaction such as abundant accretionary lapilli (e.g., Porritt et al., 2009; Porritt and Russell, 2012), however these features are not universal in the deposits of basaltic maar volcanoes and their diagnostic value remains unclear.

A common counter argument against a phreatomagmatic model for kimberlite diatremes is that it would apparently require all kimberlites to erupt via phreatomagmatic mechanisms, implying in turn that all kimberlite magmas erupt to form pipes/diatremes (e.g., Sparks et al., 2006; Cas et al., 2008). With this perspective, the phreatomagmatic model seems like special pleading, since no other magma type on Earth has been observed to only erupt phreatomagmatically. This argument can be turned around: no other small volume, basic or ultrabasic magma type on Earth has been documented to form large diatremes via purely magmatic-volatile driven mechanisms, especially those of Plinian scale (as has been suggested for kimberlites, Sparks et al., 2006; Porritt et al, 2008). The material presented here suggests that it is probably not the case that all kimberlite eruptions form large diatremes, but rather that this perspective results from biases introduced by erosion of volcanic terrains, by site selection for

mining activity, and by underreporting of small features such as dikes. Our dataset and observations from numerous kimberlite fields suggests that kimberlite magmas erupt in a variety of ways. This is consistent with other magma types whose eruptive style is dependent on processes intrinsic to magma ascent (ascent speed, gas content, degassing history, and cooling rate) as well as environmental conditions (presence or absence of ground or surface water). In the absence of abundant data on the surface expression of kimberlite volcanoes with which to draw evidence on eruption style, we could benefit from looking to intraplate basaltic and ultramafic volcanic fields (e.g., Lake Natron-Engaruka monogenetic field, Mattsson and Tripoli, 2011; Hopi Buttes field, White, 1991). Despite differences in detail, such as the inferred high gas contents and low melt viscosities and of kimberlite magmas, there are many similarities with other more common volcanoes that can be explored.

Conclusions

The geological record, selective mining, and underreporting of dikes present a biased view of kimberlite volcanism. This bias is foremost a result of erosion that removes the products of eruptive activity that disrupts little country rock during ascent and leaves most of its record on the Earth's surface, and favors preservation of eruptions that disrupt large volumes of country rock and leave much of their record below the surface. We suggest that our current view of kimberlite volcanism is skewed by this bias and by the collection of most geological data from a very small sample composed of the largest known kimberlite pipes. There is a compelling correlation between the maximum size (area) of a kimberlite pipe in a field and the estimated amount of erosion that that field has experienced since emplacement that warrants further investigation. This may suggest that there is a maximum size that a kimberlite pipe can reach (~500 m diameter at ~200 m depth). The surface and subsurface expression and inferred eruptive products of kimberlite volcanism may be comparable in magnitude and dynamics to small monogenetic basaltic eruptions that are driven by magmatic, phreatomagmatic, and combined eruption mechanisms. In order to understand the full expression of kimberlite volcanism, we recommend that research efforts be turned towards the description and interpretation of small kimberlite bodies (e.g., dikes and small kimberlite pipes) as well as the shallow subsurface plumbing systems of other monogenetic mafic and ultrabasic volcanoes.

Acknowledgements

We thank Johann Stiefenhofer and Hielke Jelsma (De Beers), Shawn Harvey and George Read (Shore Gold Inc.), Wayne Pettit and Jon Carlson (BHP Billiton) and Don Duncan (Savannah Diamonds) for generously supplying proprietary data on kimberlite fields and for permission to publish. We thank

590 Claire Palmer for providing access to publications and for discussion. Lucy Porritt and Volker Lorenz
591 are thanked for detailed helpful reviews and Michael Ort and Nancy Riggs are thanked for reviews and
592 editorial stewardship. RJB thanks Matthew Field and Kelly Russell for their many useful discussions
593 and comments. The ideas expressed in this paper are solely those of the authors.
594
595 **References**
596 Auer, A., Martin, U., Németh, K. 2007. The Fekete-hegy (Balaton Highland Hungary) "soft-substrate"
597 and "hard-substrate" maar volcanoes in an aligned volcanic complex – Implications for vent geometry,
598 subsurface stratigraphy and the paleoenvironmental setting. J. Volcanol. Geotherm. Res., 159, 225–
599 245.
600
601 Barnett, W.P., 2004. Subsidence breccias in kimberlite pipes- an application of fractal analysis. Lithos,
602 76, 299–316.
603
604 Barnett, W.P., 2008. The rock mechanics of kimberlite volcanic pipe excavation. J. Volcanol.
605 Geotherm. Res. 174, 29–39.
606
607 Basson, I.J., and Viola, G., 2003. Structural overview of selected Group II kimberlite dyke arrays in
608 South Africa: implications for kimberlite emplacement mechanisms: South African Journal of
609 Geology, 106, 375–394, doi: 10.2113/106.4.375.
610
611 Beget. J.E., Hopkins, D.M., Charron, S.D., 1996. The largest known maars on Earth, Seward
612 Peninsula, northwest Alaska. Arctic, 49, 62–69.
613
614 Belousov, A.B., 2006. Distribution and eruption mechanism of maars in the Kamchatka Peninsula.
615 Doklady Earth Sci., 406, 24–27.
616
617 Berg, G.W.,Carlson, J.A., 1998. The Leslie kimberlite pipe of Lac de Gras, Northwest Territories,
618 Canada: Evidence for near surface hypabyssal emplacement. Extended Abstracts 7th International
619 Kimberlite Conference, Cape Town, 81–83.
620
621 Berryman, A., Scott Smith, B.H., Jellicoe, B., 2004. Geology and diamond distribution of the 140/141
622 kimberlite, Fort à la Corne, central Saskatchewan, Canada. Lithos, 76, 99–114.

Blaikie, T.N., Ailleres, L., Cas, R.A.F., Betts, P.G., 2012. Three-dimensional potential field modeling of a multi-vent maar-diatreme – The Lake Coragulac maar, Newer Volcanics Provice, south-eastern Australia. J. Volcanol. Geotherm. Res., 235–236, 70–83.

Brown, R.J., Kavanagh, J., Sparks, R.S.J., Tait, M., Field, M., 2007. Mechanically disrupted and chemically weakened zones in segmented dike systems cause vent localization: Evidence from kimberlite volcanic systems. Geology 35, 184–188.

Brown, R.J., Buse, B., Sparks, R.S.J., Field, M., 2008a. On the welding of pyroclasts from very low–viscosity magmas: Examples from kimberlite volcanoes. J. Geol.116, 354–374.

Brown, R.J., Gernon, T., Stiefenhofer, J., Field, M., 2008b. Geological constraints on the eruption of the Jwaneng Central kimberlite pipe, Botswana. J. Volcanol. Geotherm. Res. 174, 195–208.

Brown, R.J., Tait, M., Field, M., Sparks, R.S.J., 2009. Geology of a complex kimberlite pipe (K2 pipe, Venetia mine, South Africa): Insights into conduit processes during explosive ultrabasic eruptions. Bull. Volcanol. 71, 95–112.

Brown, R.J., Manya, S., Buisman, I., Field, M., Fontana, G., Mac Niocaill, C., Sparks, R.S.J., Stuart, F.N., 2012. Eruption of Kimberlite Magmas: Physical volcanology, Geomorphology, and Age of the Youngest Kimberlitic Volcanoes known on Earth (the Upper Pleistocene/Holocene Igwisi Hills volcanoes, Tanzania). Bull. Volcanol. 74, 1621–1643.

Carn, S., 2000. The Lamongan volcanic field, East Java, Indonesia: physical volcanology, historic activity and hazards. J. Volcanol. Geotherm. Res. 95, 81–108.

Cas, R.A.F., Wright, J.V., 1987. Volcanic successions modern and ancient. Allen & Unwin, London, 487 pp.

Cas, R.A.F., Hayman, P., Pittari, A., Porritt, L., 2008. Some major problems with existing models and terminology associated with kimberlite pipes from a volcanological perspective, and some suggestions. J. Volcanol. Geotherm. Res. 174, 209–225.

Clement, C.R., 1982. A comparative geological study of some major kimberlite pipes in northern Cape and Orange Free State. PhD thesis (unpublished) University of Cape Town, pp 432.

Condit, C.D., Connor, C.B., 1996. Recurrence rates of volcanism in basaltic volcanic fields: An example from the Springerville volcanic field, Arizona: Geol. Soc. Am. Bull. 108, 1225–1241.

Connor, C.B., Conway, F.M., 2000. Basaltic volcanic fields. In: Sigurdsson, H. (Ed.), Encyclopedia of Volcanoes, Academic Press, New York, pp. 331–343.

Conway, F.M., Ferrill, D.A., Hall, C.M., Morris, A.P., Stamatakos, J.A., Connor, C.B., Halliday, A.N., Condit, C., 1997. Timing of basaltic volcanism along the Mesa Butte Fault in the San Francisco Volcanic Field, Arizona, from $^{40}Ar/^{39}Ar$ dates: Implications for longevity of cinder cone alignments. J. Geophys. Res. 102, 815–824.

Dawson, J.B., 1970. The structural setting of African kimberlite magmatism. In: Clifford, T.N., Gass, I.G. (Eds.), African magmatism and tectonics. Oliver and Boyd, Edinburgh, pp. 321–335.

Dawson, J.B., Hawthorne, J.B., 1973. Magmatic sedimentation and carbonatitic differentiation in kimberlite sills at Benfontein, South Africa. J. Geol. Soc. London 129, 61–85.

Dawson, J.B., 1994. Quaternary kimberlitic volcanism on the Tanzania craton. Contrib. Min. Pet. 116, 473–485.

Delaney, P.T., Pollard, D.D., 1981. Deformation of host rocks and flow of magma during growth of Minette dikes and breccia-bearing intrusions near Ship Rock, New Mexico. US Geol. Surv. Prof. Paper 1202, pp 60.

Delaney, P.T., Gartner, A.E., 1997. Physical processes of shallow mafic dike emplacement near the San Rafael Swell, Utah. Geol. Soc. Am. Bull. 109, 1177–1192.

687 Dempster, A.N., Tucker, R., 1973. The geology of the Sekameng (Buthe-Buthe) kimberlite pipe and
688 the associated dyke swarm. In: Nixon, P.H., (Ed), 1973. Lesotho Kimberlites. Lesotho National
689 Development Corporation, 180–189.
690
691 Doubik, P., Hill, B.E., 1999. Magmatic and hydromagmatic conduit development during the 1975
692 Tolbachik eruption, Kamchatka, with implications for hazards assessment at Yucca Mountain, NV. J.
693 Volcanol. Geotherm. Res. 91, 43-64.
694
695 Eley, R., Grütter, H., Louw, A., Tunguno, C., Twidale, J., 2008. Exploration Geology of the Luxinga
696 Kimberlite Field (Angola) with Evidence Supporting the Presence of Kimberlite Lava. Extended
697 Abstract, 9th Int. Kimberlite Conf., Frankfurt, Germany.
698
699 Field, M., Gibson, J.G., Wilkes, T.A., Gababotse, J., Khutjwe, P., 1997. The geology of the Orapa
700 A/K1 Kimberlite, Botswana: further insight into the emplacement of kimberlite pipes. In: Dobretsov,
701 N.L., Goldin, S.V., Kontorovich, A.E., Polyakov, G.V., Sobolev, N.V., (Eds), Proceedings of the Sixth
702 International Kimberlite Conference, Novosibirsk, Russia: Kimberlites, Related Rocks and Mantle
703 Xenoliths. Russian Geology and Geophysics, 38/1, 24–39.
704
705 Field, M., Scott Smith, B.H., 1999. Contrasting geology and near–surface emplacement of kimberlite
706 pipes in southern Africa and Canada. In: Gurney, J., Gurney, J., Pascoe, M., Richardson, S. (Eds.),
707 Dawson J.B. Proceedings of the VII International Kimberlite Conference. Vol. 1, Red Roof design cc,
708 Cape Town, 214–237.
709
710 Field, M., Stiefenhofer, J., Robey, J., Kurszlaukis, S., 2008. The kimberlite–hosted diamond deposits of
711 southern Africa: a review. Ore Geol. Rev., 34, 33–75.
712
713 Fontana, G., Mac Nio Caill, C., Brown, R.J., Sparks, R.S.J., Field, M., 2011. Emplacement
714 temperatures of pyroclastic and volcaniclastic deposits in kimberlite pipes in southern Africa. Bull.
715 Volcanol., 73, 1063–1083.
716
717 Gaffney, E.S., Damjanac, B., Valentine, G.A., 2007. Localization of volcanic activity: 2.Effects of pre-
718 existing structure. Earth Planet. Sci. Lett. 263, 323-338, doi: 10.1016/j.epsl.2007.09.002.
719

Gernon, T., Sparks, R.S.J., Field, M., 2008. Degassing structures in volcaniclastic kimberlite: examples from southern African pipes. J. Volcanol. Geotherm. Res. 174, 186–194.

Gernon, T.M., Fontana, G., Field, M., Sparks, R.S.J., Brown, R.J., Mac Niocaill, C., 2009a. Pyroclastic flow deposits from a kimberlite eruption: the Orapa south crater, Botswana. Lithos, 112, 566–578.

Gernon, T.M., Fontana, G., Field, M., Sparks, R.S.J., 2009b. Depositional processes in a kimberlite crater: the Upper Cretaceous Orapa South Pipe (Botswana). Sedimentology, 56, 623–643.

Gernon, T.M., Field, F., Sparks, R.S.J., 2012. Geology of the Snap Lake kimberlite intrusion, Northwest Territories, Canada: Field observations and their interpretation. J. Geol. Soc., 169, 1–16.

Geshi, N., Kusumoto, S., Gudmundsson, A., 2010. Geometric difference between non-feeder and feeder dikes. Geology, 38, 195-198, doi: 10.1130/G30350.1

Goto, A., Taniguchi, H., Yoshida, M., Ohba, T., Oshima, H., 2001. Effects of explosion energy and depth to the formation of blast wave and crater: Field explosion experiment for the understanding of volcanic explosion. Geophysic. Res. Lett., 28, 4287–4290.

Gurney, J.J., Kirkley, M.B., 1996. Kimberlite dike mining in South Africa. Spec. Ed. Africa Geosci., Rev., 35–45.

Gutmann, J.T., 2002. Strombolian and effusive activity as precursors to phreatomagmatism: eruptive sequence at maars of the Pinacate volcanic field, Sonora, Mexico. J. Volcanol. Geotherm. Res. 113, 345–356.

Haggerty, S.E., 1982. Kimberlites in Western Liberia: an overview of the geological setting in a plate tectonic framework. J. Geophys. Res. 87, 10811–10826.

Hanson, E.K., Moore, J.M., Bordy, E.M., Marsh, J.S., Howarth, G., Robey, J.V.A., 2009. Cretaceous erosion in central South Africa: evidence from upper-crustal xenoliths in kimberlite diatremes. South Africa J. Geol. 112, 125–140.

753 Hare, A.G., Cas, R.A.F., 2005. Volcanology and evolution of the Werribee Plains intraplate, basaltic
754 lava flow-field, Newer Volcanics Province, southeast Australia. Aus. J. Earth Sci. 52, 59–78.
755
756 Harvey, S., Kjarsgaard, B., McClintock, M., Shimell, M., Fourie, L., Du Plessis, P., Read, G., 2009.
757 Geology and evaluation strategy of the Star and Orion South kimberlites, Fort à la Corne, Canada.
758 Lithos, 112, 47–60
759
760 Hasenaka.T., Carmichael, I.S.E., 1985. The cinder cones of Michoacan-Guanajuato, Central Mexico:
761 their age, volume and distribution, and magma discharge rate. J. Volcanol. Geotherm. Res., 25, 105–
762 124.
763
764 Hawthorne, J.B., 1975. Model of a kimberlite pipe. Phys. Chem. Earth 9, 1–15.
765
766 Hintz, A.R., Valentine, G.A., 2012. Complex plumbing of monogenetic scoria cones: New insights
767 from the Lunar Crater Volcanic Field (Nevada, USA). J. Volcanol. Geotherm. Res., 239-240, 19–32.
768
769 Hirano, N., Takahashi, E., Yamamoto, J., Abe, N., Ingle, S.P., Kaneoka, I., Hirata, T., Kimura, J.-I.,
770 Ishii, T., Ogawa, Y., Machida, S., and Suyehiro, K., 2006. Volcanism in response to plate flexure:
771 Science, 313, 1426–1428 and online supplemental material.
772
773 Houghton, B.F., Wilson, C.J.N., Smith, I.E.M., 1999. Shallow-seated controls on styles of explosive
774 basaltic volcanism: a case study from New Zealand. J. Volcanol. Geotherm. Res. 91, 97–120.
775
776 Jelsma, H.A., de Wit, M.J., Thiart, C., Dirks, P.H.G.M., Viola, G., Basson, I.J., Anckar, E., 2004.
777 Preferential distribution along transcontinental corridors of kimberlites and related rocks of southern
778 Africa. South African J. Geol. 107, 301–324.
779
780 Jelsma, H.A., de Wit, M.J., Thiart, C., Dirks, P.H.G.M., Viola, G., Basson, I.J., Anckar, E., 2004.
781 Preferential distribution along transcontinental corridors of kimberlites and related rocks of southern
782 Africa. South African J. Geol. 107, 301–324.
783
784 Kavanagh, J.L., Menand, T., Sparks, R.S.J., 2006. An experimental investigation of sill formation and
785 propagation in layered elastic media. Earth Planet. Sci. Lett., 245, 799–813.

Kavanagh, J.L., Sparks, R.S.J., 2011. Insights of dyke emplacement mechanics from detailed 3D dyke thickness datasets. J. Geol. Soc. London, 168, 965–978.

Keating, G.N., Valentine, G.A., Krier, D.J., Perry, F.V., 2008. Shallow plumbing systems for small-volume basaltic volcanoes. Bull. Volcanol. 70, 563–582.

Kirkley, M.B., Kolebaba, M.R., Carlson, J.A., Gonzales, A.M., Dyck, D.R., Dierker, C., 1998. Kimberlite emplacement processes interpreted from Lac de Gras examples. Extended Abstracts, 7th International Kimberlite Conference, Cape Town 429-431.

Kjarsgaard, B.A., 1996. Kimberlite-hosted diamond. In: Eckstrand, O.R., Sinclair, W.D., Thorpe, R.I. (Eds.), Geology of Canadian Mineral Deposit Types. Geol. Surv. Canada, 8, 560–568.

Kjarsgaard, B.A., 2007. Kimberlite diamond deposits. In: Goodfellow, W.D., Ed., Mineral Deposits of Canada: A Synthesis of Major Deposit Types, District Metallogeny, the Evolution of Geological Provinces, and Exploration Methods: Geological Association of Canada, Mineral Deposits Division, Special Publication 5, 245–272.

Kjarsgaard, B.A., Harvey, S., McClintock, M., Zonneveld, J.P., Du Plessis. P., McNeil, D., Heaman, L., 2009. Geology of the Orion South kimberlite, Fort à la Corne, Canada. Lithos 1125, 600–617.

Kresten, P., Dempster, A.N., 1973. The Geology of Pipe 200 and the Malibamatso dyke swarm. In: Nixon, P.H., (Ed), 1973. Lesotho Kimberlites. Lesotho National Development Corporation, 172–179.

Kuntz, M.A., Champion, D.E., Spiker, E.C., LeFebvre, R.H., 1986. Contrasting magma types and steady-state, volume-predictable basaltic volcanism along the Great Rift, Idaho. Geol. Soc. Am. Bull. 97, 579-594.

Kurszlaukis, S., Barnett, W.P., 2003. Volcanological and structural aspects of the Venetia Kimberlite field – a case study of South African kimberlite maar-diatreme volcanoes. South African J. Earth Sci. 106, 165–192.

819 Kurszlaukis, S., Mahotkin, I., Rotman, A.Y., Kolesnikov, G.V., Makovchuk, I.V., 2009. Syn- and post-
820 eruptive volcanic processes in the Yubileinaya kimberlite pipe, Yakutia, Russia, and implications for
821 the emplacement of South African-style kimberlite pipes. Lithos 112, 579–591.
822
823 Leckie, D.A., Kjarsgaard, B.A., Bloch, J., McIntyre, D., McNeil, D., Stasiuk, L., Heaman, L., 1997.
824 Emplacement and reworking of Cretaceous, diamond-bearing, crater facies kimberlite of central
825 Saskatchewan, Canada. Geol. Soc. Am. Bull. 109, 1000–1020.
826
827 Lefebvre, N., Kurszlaukis, S., 2008. Contrasting eruption styles of the 147 Kimberlite, Fort à la Corne,
828 Saskatchewan, Canada. J. Volcanol. Geotherm. Res., 174, 171–185.
829
830 Lesti, C., Giordano, G., Salvini, F., Cas, R.A.F., 2008. Volcano tectonic setting of the intraplate,
831 Pliocene-Holocene, Newer Volcanic Province (southeast Australia): Role of crustal fracture zones. J.
832 Geophys. Res. 113, B07407, doi:10.1029/2007JB005110.
833
834 Lockhart, G., Grütter, H., Carlson, J., 2004. Temporal, geomagnetic and related attributes of kimberlite
835 magmatism at Ekati, Northwest territories, Canada. Lithos, *77*, 665–682.
836
837 Lorenz, V., 1975. Formation of phreatomagmatic maar-diatreme volcanoes and its relevance to
838 kimberlite diatremes. Phys. Chem. Earth 9, 17–27.
839
840 Lorenz, V., 1979. Phreatomagmatic origin of the olivine melilitite diatremes of the Swabian Alb, Germany. In:
841 Boyd, F.R. & Meyer, H.O.A. (Eds.): Kimberlites, diatremes and diamonds: their geology, petrology and
842 geochemistry. Proc. Sec. Int. Kimberlite Conf., 1, 354-363, Amer. Geophys. Union, Washington, USA.
843
844 Lorenz, V., 1986. On the growth of maars and diatremes and its relevance to the formation of tuff
845 rings. Bull. Volcanol., 48, 265–290.
846
847 Lorenz, V., Büchel, G., 1980. Zur Vulkanologie der Maare und Schlackenkegel der Westeifel.
848 Mitteilungen der Pollichia, 68, 29–100.
849

Lorenz, V., Kurszlaukis, S., 2007. Root zone processes in the phreatomagmatic pipe emplacement model and consequences for the evolution of maar-diatreme volcanoes. J. Volcanol. Geotherm. Res. 159, 4–32.

Mainkar, D., Lehmann, B., Haggerty, S.E., 2004. The crater–facies kimberlite system of Tokapal, Bastar district, Chhattisgarh, India. Lithos, 76, 201–217.

Marsh, J., 1973. Relationships between transform directions and alkaline igneous rock lineaments in Africa and South America. Earth Planet. Sci Lett., 18, 317–323.

Martin, U., Németh, K., 2005. Eruptive and depositional history of a Pliocene tuff ring that developed in a fluvio-lacustrine basin: Kissomlyó volcano (western Hungary). J. Volcanol. Geotherm. Res. 147, 342–356.

Matthes, H., Kroner, C., Jahr, T., Kampf, H., 2010. Geophysical modeling of the Ebersbrunn diatreme, western Saxony, Germany. Near Surface Geophys., 8, 311–319.

Mattsson, H.B., Tripoli, B.A., 2011. Depositional characteristics and volcanic landforms in the lake Natron-Engaruka monogenetic field, northern Tanzania. J. Volcanol. Geotherm. Res., 203, 23–34.

Mazzarini, F., D'Orazio, M., 2003. Spatial distribution of cones and satellite-detected lineaments in the Pali Aike Volcanic Field (southernmost Patagonia): insights into the tectonic setting of a Neogene rift system. J. Volcanol. Geotherm. Res. 125, 291–305.

McClintock, M., White, J.D.L., Houghton, B.F., Skilling, I.P., 2008. Physical volcanology of a large crater-complex formed during the initial stages of Karoo flood basalt volcanism, Sterkspruit, Eastern Cape, South Africa. J. Volcanol. Geotherm. Res. 172, 93–111.

McGetchin, T.R., Ullrich, G.W., 1973. Xenoliths in maars and diatremes with inferences for the Moon, Mars, and Venus. J. Geophys. Res. 78, 1833–1853.

Mitchell, R.H., 1986. Kimberlites. Mineralogy, Geochemistry and Petrology. Plenum Press 442 p.

Moore, A., Blenkinsop, T., Cotterill, F., 2008. Controls on post-Gondwana alkaline volcanism in Southern Africa. Earth Planet. Sci. Lett. 268, 151–164.

Moss, S., Russell, J.K., Brett, R.C., Andrews, G.D.M., 2009. Spatial and temporal evolution of kimberlite magma at A154N, Diavik, Northwest Territories, Canada. Lithos, 112, 541–552.

Nixon, P.H., 1973. How wide, how long, what shape? The vital statistics of Lesotho kimberlites. Unpublished report: Department of mines and geology, Lesotho, PHN/16.

Nixon, P.H., 1995. The morphology and nature of primary diamondiferous occurrences. J. Geochem. Ex. 53, 41–71.

Nowicki, T., Crawford, B., Dyck, D., Carlson, J., McElroy, R., Oshust, P., Helmstaedt, H., 2004. The geology of kimberlite pipes of the Ekati property, Northwest Territories, Canada. Lithos 76, 1–27.

Pettit, W., 2009. Geophysical signatures of some recently discovered large (N40 ha) kimberlite pipes on the Alto Cuilo concession in north-eastern Angola. J. Volcanol. Geotherm. Res., 112:106–115.

Pirrung, M., Büchel, G., Lorenz, V., Treutler, H-., 2008. Post–eruptive development of the Ukinrek east maar since its eruption in 1977 A.D. in the periglacial area of south–west Alaska. Sedimentology 55, 305–334.

Pittari, A., Cas, R.A.F., Lefebvre, N., Robey, J., Kurszlaukis, S., Webb, K. 2008. Eruption processes and facies architecture of the Orion Central kimberlite volcanic complex, Fort à la Corne, Saskatchewan; kimberlite mass flow deposits in a sedimentary basin. J. Volcanol. Geotherm. Res., 174, 152–170.

Porritt, L.A., Cas, R.A.F., Crawford, B., 2008. In-vent column collapse as an alternative model for massive volcaniclastic kimberlite emplacement: An example from the Fox kimberlite, Ekati Diamond Mine, NWT, Canada. J. Volcanol. Geotherm. Res., 174, 90–102.

914 Porritt. L.A., Cas, R.A.F., 2009. Reconstruction of a kimberlite eruption, using an integrated
915 volcanological, geochemical and numerical approach: A case study of the Fox Kimberlite, NWT,
916 Canada. J. Volcanol. Geotherm. Res. 179, 241–264.
917
918 Porritt, L.A., Russell, J.K., 2012. Kimberlite ash: fact or fiction? Phys. Chem. Earth, 45–46, 24–32.
919
920 Robles-Cruz, S.E., Watangua, M., Isidoro, L., Melgarejo, J.C., Galí, S., Olimpio, A., 2009. Contrasting
921 compositions and textures of ilmenite in the Catoca kimberlite, Angola, and implications in exploration
922 for diamond. Lithos, 112, 966–975.
923
924 Rolfe, D.G., 1973. The geology of the Kao kimberlites. In: Nixon, P.H., 1973. Lesotho Kimberlites,
925 Lesotho National Development Corporation, 101-105.
926
927 Rombouts, L., 1987. Geology and evaluation of the Guinean diamond deposits. Annales de la Société
928 Géologique de Belgique, 110, 241–259.
929
930 Ross, P.-S., White, J.D.L., 2006. Debris jets in contintental phreatomagmatic volcanoes: A field study
931 on their subterranean deposits in the Coombs Hill vent complex, Antarctica: J. Volcanol. Geotherm.
932 Res., 149, 62–84.
933
934 Ross, P.-S., White, J.D.L., Zimanowski, B., Büttner, R., 2008a. Multiphase flow above explosion sites
935 in debris-filled volcanic vents: Insights from analogue experimens: J. Volcanol. Geotherm. Res., 178,
936 104–112.
937
938 Ross, P.-S., White, J.D.L., Zimanowski, B., Büttner, R., 2008b. Rapid injection of particles and gas
939 into non-fluidized granular material, and some volcanological implications. Bull. Volcanol., 70, 1151–
940 1168, doi: 10.1007/s00445-008-0230-1.
941
942 Ross, P–S., Delpit, S., Haller, M.J., Németh, K., Corbella, H., 2011. Influence of the substrate on maar-
943 diatreme volcanoes—an example of a mixed setting from the Pali Aike volcanic field, Argentina. J.
944 Volcanol. Geotherm. Res. 201, 253–271.
945

946 Russell, J.K., Porritt, L.A., Lavallee, Y., Dingwell, D.B., 2012. Kimberlite ascent by assimilation-
947 fuelled buoyancy. Nature, 481, 352–356.
948
949 Schmincke, H-U., 2007. The Quaternary volcanic fields of the East and West Eifel (Germany). In:
950 Ritter, R., Christensen, U., (Eds) Mantle plumes-a multidisciplinary approach. Springer-Heidelberg, pp
951 241.
952
953 Skinner, E.M.W., Marsh, J.S., 2004. Distinct kimberlite pipe classes with contrasting eruption
954 processes. Lithos 76, 183–200.
955
956 Smith, E.I., Sánchez, A., Walker, J., Wang, K., 1999. Geochemistry of mafic magmas in the Hurricane
957 volcanic field, Utah: Implications for small- and large-scale chemical variability of the lithospheric
958 mantle: J. Geol., 107, 433–448.
959
960 Smith, I.E.M., Blake, S., Wilson, C.J.N., Houghton, B.J., 2008. Deep-seated fractionation during the
961 rise of a small-volume basalt magma batch: Crater Hill, Auckland, New Zealand. Contrib. Mineral.
962 Petrol. 155, 511–527.
963
964 Snyder, D.B., Lockhart, G.D., 2005. Kimberlite trends in NW Canada. J. Geol. Soc. London, 162, 737–
965 740.
966
967 Sottili, G., Palladino, D.M., Gaeta, M., Masotta, M., 2012. Origins and energetics of maar volcanoes:
968 examples from the ultrapotassic Sabatini Volcanic District (Roman Province, Central Italy). Bull.
969 Volcanol., 74. 163–186. doi: 10.1007/s00445-011-0506-8.
970
971 Sparks, R.S.J., Baker, L., Brown, R.J., Field, M., Schumacher, J., Stripp, G., 2006. Dynamical
972 constraints on kimberlite volcanism. J. Volcanol. Geotherm. Res. 155, 18–48.
973
974 Stiefenhofer, J., Farrow, D.J., 2004. Geology of the Mwadui kimberlite, Shinyanga district, Tanzania.
975 Lithos, 76, 139–160.
976
977 Sudo, M., Uto, K., Tatsumi, Y., Matsui, K., 1998. K-Ar geochronology of a Quaternary monogenetic
978 volcano group in Ojika Jima District, Southwest Japan. Bull. Volcanol. 60, 171–186.

Taddeucci, J., Sottili, G., Palladino, D.M., Ventura, G., Scarlato, P., 2010. A note on maar eruption energetics: current models and their application. Bull. Volcanol. 72, 75–83, doi:10.1007/s00445-009-0298-2.

Valentine, G.A., 2012. Shallow plumbing systems for small-volume basaltic volcanoes, 2: Evidence from crustal xenoliths at scoria cones and maars. J. Volcanol. Geotherm. Res., 223–224, 47–63, doi:10.1016/j.jvolgeores.2012.01.012.

Valentine, G.A., Groves, K.R., 1996. Entrainment of country rock during basaltic eruptions of the Lucero volcanic field, New Mexico. J. Geol., 104, 71–90.

Valentine, G.A., Krogh, K.E.C., 2006. Emplacement of shallow dikes and sills beneath a small basaltic volcanic center – The role of pre-existing structure (Paiute Ridge, southern Nevada, USA). Earth Planet. Sci Letts. 246, 217–230.

Valentine, G.A., Perry, F.V., 2006. Decreasing magmatic footprints of individual volcanoes in a waning basaltic field. Geophys. Res. Lett. 33, L14305.doi:10.1029/2006GL026743.

Valentine, G.A., Keating, G.N., 2007. Eruptive styles and inferences about plumbing systems at Hidden Cone and Little Black Peak scoria cone volcanoes (Nevada, U.S.A.). Bull. Volcanol., 70, 104–113. doi:10.1007/s00445-007-0123-8.

Valentine, G.A., Perry, F.V., 2007. Tectonically controlled, time-predictable basaltic volcanism from a lithospheric mantle source (central Basin and Range Province, USA). Earth Planet. Sci. Lett., 261, 201–216. doi:10.1016/j.epsl.2007.06.029.

Valentine, G.A., White, J.D.L., 2012. Revised conceptual model for maar-diatremes: subsurface processes, energetics, and eruptive products. Geology, doi: 10.1130/G33411.1.

Valentine, G.A., Krier, D.J., Perry, F.V., Heiken, G., 2007. Eruptive and geomorphic processes at the Lathrop Wells scoria cone volcano. J. Volcanol. Geotherm. Res., 161, 57–80. doi:10.1016/j.jvolgeores.2006.11.003.

Valentine, G.A., Shufelt, N.L., Hintz, A.R.L., 2011. Models of maar volcanoes, Lunar Crater (Nevada, USA). Bull. Volcanol. 73, 753–765, doi: 10.1007/s00445.011-0451-6.

Vearncombe, S., Vearncombe, J.R., 2002. Tectonic controls on kimberlite location, South Africa. J. Structural Geol. 24, 1619–1625.

Walters, A.L., Phillips, J.C., Brown, R.J., Field, M., Gernon, T., Stripp, G., 2006. The role of fluidisation in the formation of volcaniclastic kimberlite: Grain size observations and experimental investigation. J. Volcanol. Geotherm. Res. 155, 119–137.

Webb, K.J., Scott Smith, B.H., Paul, J.L., Hetman, C.M., 2004. Geology of the Victor Kimberlite, Attawapiskat, Northern Ontario, Canada: cross-cutting and nested craters. Lithos, 76, 29–50.

White, J.D.L., 1991. Maar-diatreme phreatomagmatism at Hopi Buttes, Navajo Nation (Arizona), USA. Bull. Volcanol. 53, 239–258.

White, J.D.L., Ross, P–S., 2011. Maar-diatreme volcanoes: A review. J. Volcanol. Geotherm. Res. 201, 1–29.

White, J.L., Sparks, R.S.J., Bailey, K., Barnett, W.P., Field, M., Windsor, L., 2012. Kimberlite sills and dikes associated with the Wesselton kimberlite pipe, Kimberley, South Africa. South African J. Geol. 115, 1–32.

White, S.H., de Boorder, H., Smith, C.B., 1995. Structural controls of kimberlite and lamproite emplacement. J. Geochem. Exp. 53, 245–264.

Wilson, L., Head, J.W. III., 2007. An integrated model of kimberlite ascent and eruption. Nature, 447, 53–57.

Wood, C.A., 1980. Morphometric evolution of cinder cones. J. Volcanol. Geotherm. Res. 7, 387–413.

Zonneveld, J-P., Kjarsgaard, B.A., Harvey, S.E., Heaman, L.M., McNeil, D.H., Marcia, K.Y., 2004. Sedimentologic and stratigraphic constraints on the emplacement of the Star kimberlite east–central Saskatchewan. Lithos, 76, 115–138.

Figure captions

Figure 1. Small volcanic cones of the Holocene Igwisi Hills volcanoes, Tanzania (modified from Brown et al., 2012). Surface crater diameters are <100–200 m.

Figure 2. The Fort à la Corne kimberlite field. The kimberlite field comprises pyroclastic cones and craters and is buried beneath glacial till. Larger bodies represent coalesced kimberlite deposits from two or more kimberlite volcanoes (courtesy of S. Harvey, Shore Gold Inc.).

Figure 3. Histograms and cumulative frequency curves of the areas of ~500 kimberlites from four kimberlite fields exposed at various erosion levels.

Figure 4. Kimberlite dikes and pipes in northern Lesotho (from Jelsma et al., 2009). Estimated erosion level is 300 m below paleo-surface (Hanson et al. 2009). Kimberlite pipes are circled.

Figure 5. Plot of the size of the maximum pipe in a kimberlite field against the estimated erosion level of that field. Pipes to the right of the vertical dashed line may represent flared craters and/or two or more coalesced bodies. Red arrow indicates dimensions of non-flared parts of the Orapa south and Yubileina pipes. There is a reasonably consistent decrease in maximum pipe size with erosion depth >200 m. This is comparable to that of a pipe with average wall slopes of ~80–85°. Margins of error for the amount of erosion are not well constrained and may vary from <100 m to >200 m. Grey symbols relate to pipes for which there is little geological evidence for erosion levels. The data suggest that the maximum diameter of a kimberlite pipe at around 200 m below the surface is ~500 m. At shallower depths the diameter of a pipe is dependent on flaring, which is controlled by proximity to neighboring pipes, the thickness of poorly consolidated surface rocks or sediments, and for surface deposits, the coalescence of neighboring edifices. Diameters are calculated from the diameter of equivalent area circle. [1]Pettit (2009);[2]pers comm. Shoregold Diamonds; [3]Stiefenhofer and Farrow, (2004); [4]reported in Robles-Cruz et al., 2009; [5]Field et al., 1997; [6]Nowicki et al. (2004); [7]Brown et al., (2009); [8]Kurszlaukis

et al., (2009); [9]De Beers internal report; [10]Rolfe (1973); [11]De Beers internal report; [12]Kurszlaukis and Barnett, (2003); [13]Webb et al., (2004); [14]De Beers internal report; [15]Rombouts (1987). *erosion estimates from Hanson et al., (2009).

Figure 6. Cartoon illustrating the effects of landscape erosion on the preserved record of monogenetic basaltic volcanism. A) Map and cross-section of a basaltic volcanic field comprised of scoria cones and maar volcanoes. The surface is dominated by the products of effusive and weakly explosive eruptions (scoria cones and lavas). B) Following 100–200 m of erosion, the vent structures of scoria cones have merged down into their feeder dikes, while the diatreme still has significant area extent. This results in an apparent predominance of phreatomagmatic features (diatremes) as the landscape is eroded.

Kimberlite field	[1]Age (Ma)	Over-burden	Estimated erosion level (m)	No. of pipes	Size range (10^4 m^2)	[2]d pipe (m)	No. of dikes	Country rock geology	Comments	Sources of data/references
Alto Cuilo, Angola	146–111	Kalahari sand	0	205	0.5–174	80–1500	-	Erupted into poorly consolidated to unconsolidated sediment	-	BHP Billiton data; Pettit (2009); Eley et al. (2008)
Fort à la Corne, Canada	106–98	Glacial deposits ~ 100 m thick	0	69	4–403 [largest single body = 139]	220–2300 [1350]	-	Marine sediments	Surface kimberlite volcanoes; some coalesced.	Shore Gold data: Berryman et al. (2004); Zonneveld et al., (2004)
Tanzania	189; 53	?	?<100	113	1–146	110–1360	present	? Basement	Poorly constrained dataset	Savannah Diamonds data
Orapa, Botswana	90	Kalahari sand	<<200	85	0.1–66	35–900	Present; not reported	Karoo basalt; sedimentary cover at time of eruption	-	De Beers data; Field et al. (1997); Gernon et al. (2009b)
Jwaneng, Botswana	240	Kalahari sand	<250	15	0.1–54	35–830	Present, not reported	Karoo basalt; sedimentary cover at time of eruption	-	De Beers data; Specific examples: Brown et al. (2008b)
Lesotho	Cretaceous	No	<300*	17	0.4–20	70–500	220; 21 blows	Karoo basalt lava	Exposed in mountainous highlands	Nixon (1973)
Ekati-Lac de Gras, Canada	75–43	Glacial deposits	<<500	159	0.1–16	30–450	Present (>13)	Archean metasediments and granitoids; Cretaceous Tertiary strata present at time of eruption	-	BHP Billiton data; Berg and Carlson, (1998); Carlson et al, (1998); Kirkley et al, (1998); Nowicki et al, (2004); Lockhart et al, (2004)
Kgare, Botswana	80	?Kalahari sand	<500	13	0.3–8	60–300	-	-	-	De Beers data
Venetia, South Africa	520	No	~500	15	0.1–12.5	35–400	>4	Metamorphic basement; sedimentary and volcanic rock cover.	15 kimberlite bodies in 4 km^2	Kurszlaukis and Barnett(2003); Brown et al. (2009)
Kimberley Group 1, South Africa	111–87	No	850*	68	0.1–12.7	35–400	Present; not reported	Metamorphic basement; sedimentary and volcanic rock cover	-	De Beers data; summary in Field et al. (2008)
Guinea	95	?	1000	19	0.1–9.5	35–340	Numerous	Metamorphic basement	-	Rombouts (1987)

Kimberley Group 2, South Africa	119–114	No	1250*	134	0.06–5.5	26–260	Present; not reported	Metamorphic basement; sedimentary and volcanic rock cover	-	De Beers data; summary in Field et al. (2008)

Table 1. Summary of data on kimberlite fields used in this study.[1]not all kimberlites in a field have been dated. [2]diameters of equivalent area circle.*erosion estimates from Hanson et al., (2009).

Volcanic field	Total volcanoes	% maars or tuff rings	Maar and tuff ring crater sizes	Reference
West Eifel, Germany	~240	30%	< 1700 m	Schmincke H-U (2007)
East Eifel, Germany	~100	"rare"		Schmincke H-U (2007)
Lamongan, East Java, Indonesia	~90	32%	100–800 m, "typical" ~450 m	Carn (2000)
Seward Penninsula, AK, USA	No data	No data	4000–8000 m	Beget et al. (1996)
Michoacan-Guanajuato, Mexico	1040 (43 domes, 13 shields, 22 maars/tuff rings)	2%	Not documented	Hasenaka and Carmichael (1985)
Springerville, AZ, USA	409 (5 maars, 4 fissure vents, 2 shields, several spatter mounds)	1%	Not documented	Condit and Connor (1996)
Newer Volcanic Province, Victoria, Australia	~400 (~50% scoria cones, 40% shields, 10% maars/tuff rings)	10%	1000–2000 m average diameter	Hare and Cas (2005)
Pali Aike volcanic field, Patagonia (Argentina-Chile)	139 (34 maars, remainder scoria cones)	24%	Crater diameter not provided	Mazzarini and D'Orazio (2003) – note we combined their U2 and U3 chronologic units
Pinacate volcanic field, Sonora, Mexico	400 scoria cones, 8 maars	2%	800–1600 m for 5 maars for which data are provided	Gutmann (2002)
Auckland volcanic field, New Zealand	49 basaltic centers		34 are "principally phreatomagmatic"	Houghton et al. (1999)
Hurricane volcanic field, Utah, USA	10 basaltic centers	0	All scoria cones	Smith et al. (1999)
Southwest Nevada volcanic field (Plio-Pleistocene), NV, USA	17 basaltic centers (6 buried)	0 (out of 11 exposed volcanoes)	Scoria cones and one shield	Valentine and Perry (2007)
Lunar Crater volcanic field, NV, USA	>100 basaltic centers	<5% (four likely ones in Pleistocene, plus perhaps two in older Pliocene volcanoes)		Valentine et al. (2011)
Sabatini volcanic district, Italy	45 (14 maars, remainder scoria cones)	31%	600–1700 m	Sottili et al. (2012)
Kamchatka peninsula, Russia	?>3000 (~34 maars, the rest scoria cones)	<1%	200–1600 m	Belousov (2006)

Table 2. Sizes and proportions of phreatomagmatic maars in basaltic volcanic field.

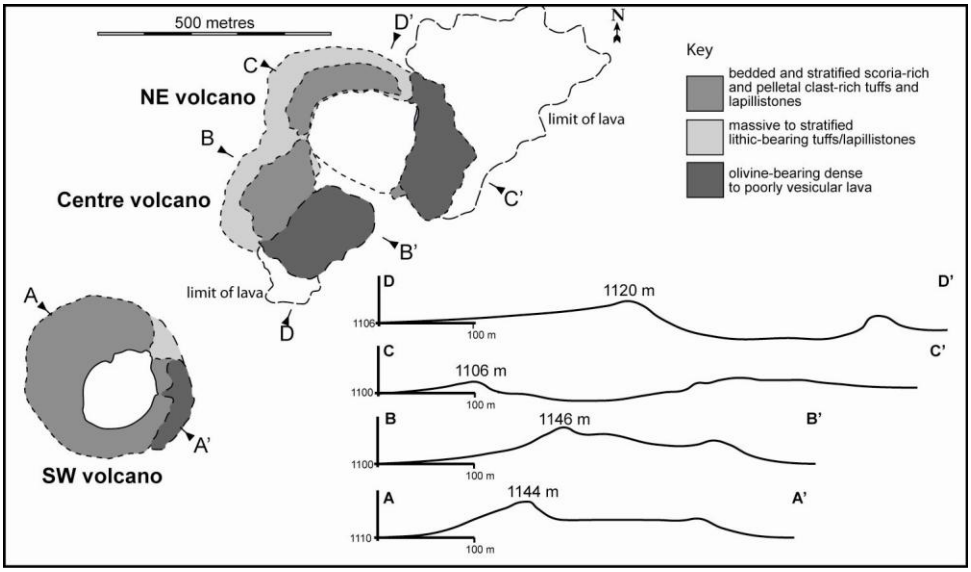
500 metres
N
D'
C
NE volcano
B
Centre volcano
B'
C'
limit of lava
A
limit of lava
D
A'
SW volcano
Key
bedded and stratified scoria-rich and pelletal clast-rich tuffs and lapillistones
massive to stratified lithic-bearing tuffs/lapillistones
olivine-bearing dense to poorly vesicular lava
D
D'
1120 m
1106
100 m
C
C'
1106 m
1100
100 m
B
B'
1146 m
1100
100 m
A
A'
1144 m
1110
100 m

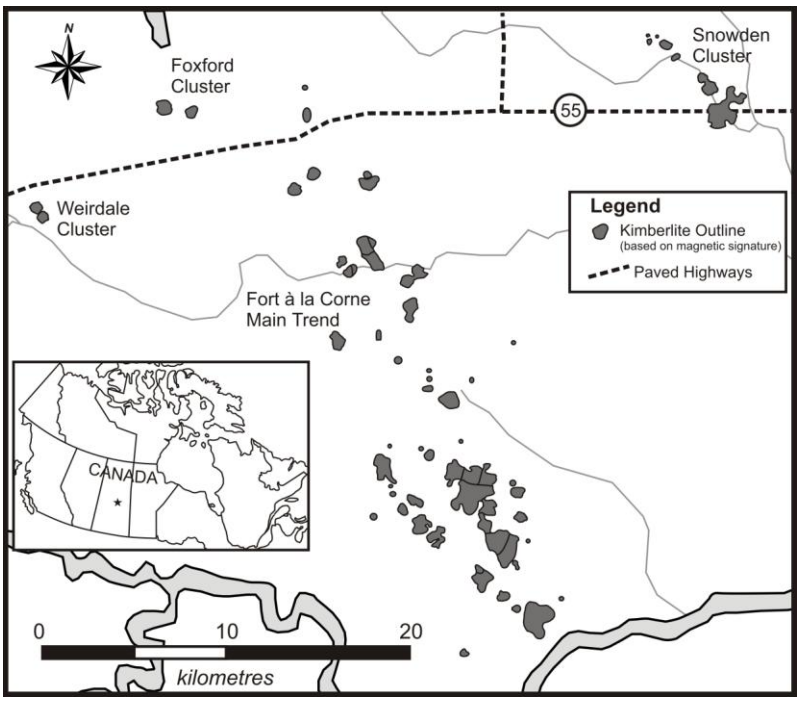
N
Foxford Cluster
Snowden Cluster
55
Weirdale Cluster
Legend
Kimberlite Outline
(based on magnetic signature)
Paved Highways
Fort à la Corne Main Trend
CANADA
0
10
20
kilometres

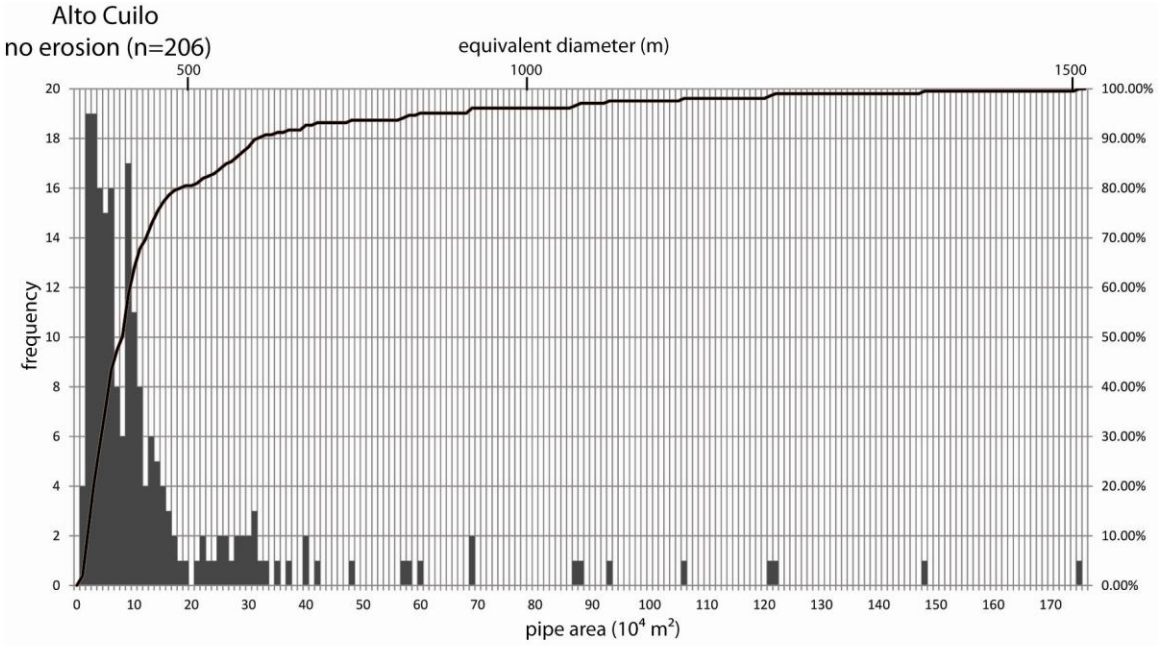
Alto Cuilo
no erosion (n=206)
equivalent diameter (m)
500
1000
1500
frequency
pipe area (10^4 m^2)

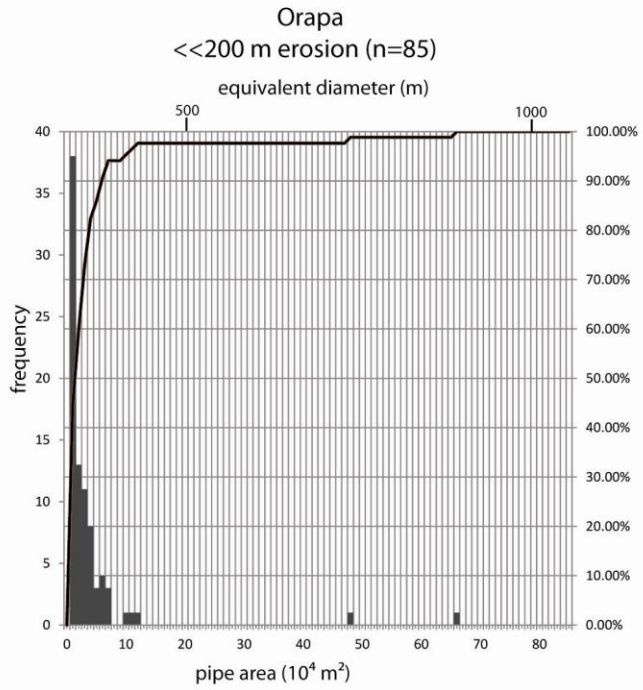
Orapa
<<200 m erosion (n=85)
equivalent diameter (m)
500
1000
frequency
pipe area (10^4 m^2)

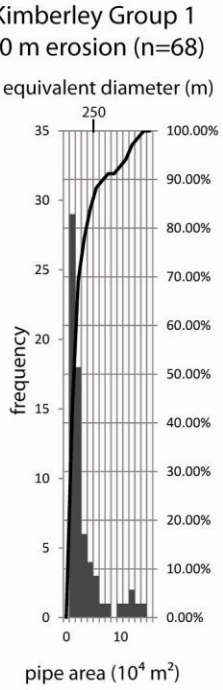
Kimberley Group 1
800 m erosion (n=68)
equivalent diameter (m)
250
frequency
pipe area (10^4 m^2)

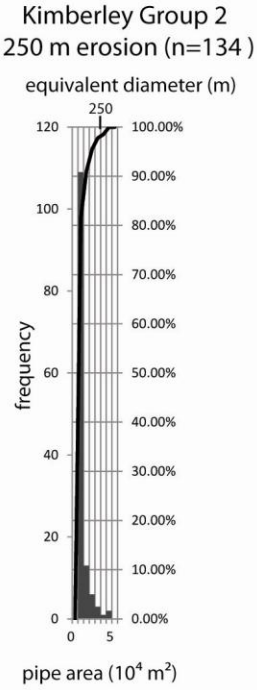
Kimberley Group 2
1250 m erosion (n=134)
equivalent diameter (m)
250
frequency
pipe area (10^4 m^2)

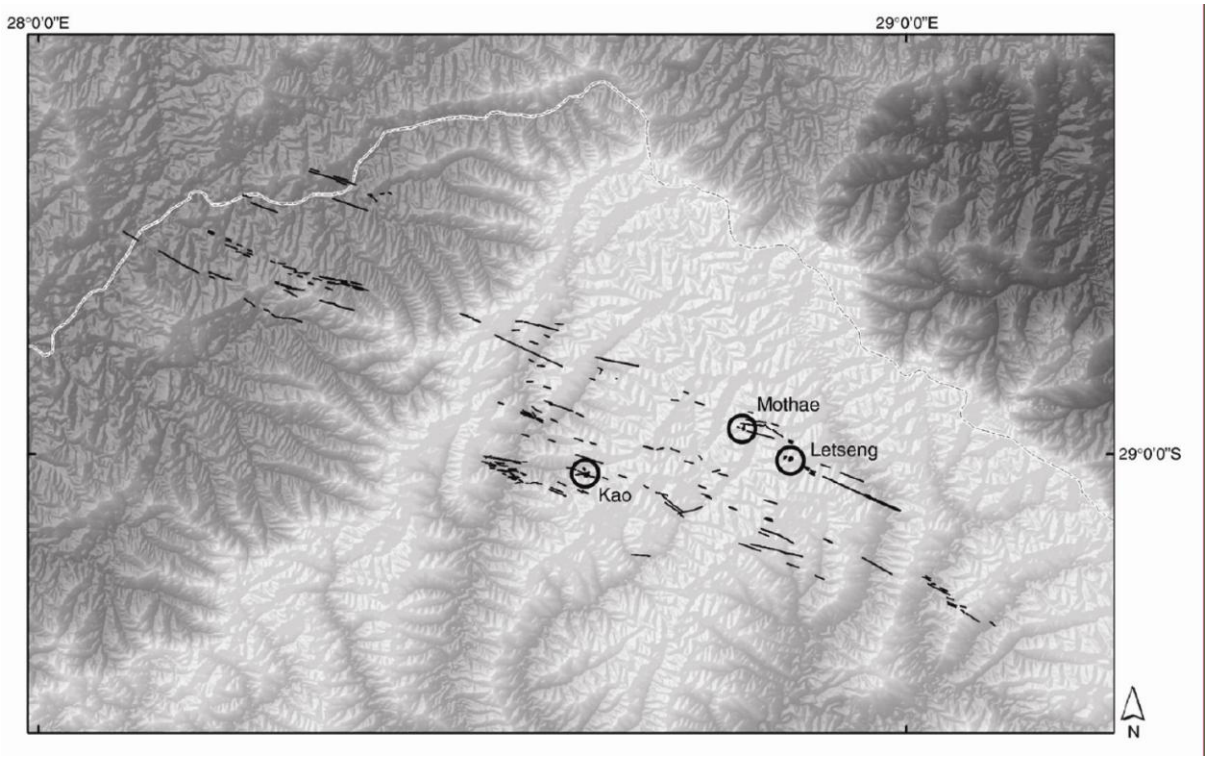
28°0'0"E
29°0'0"E
29°0'0"S
Mothae
Letseng
Kao
N

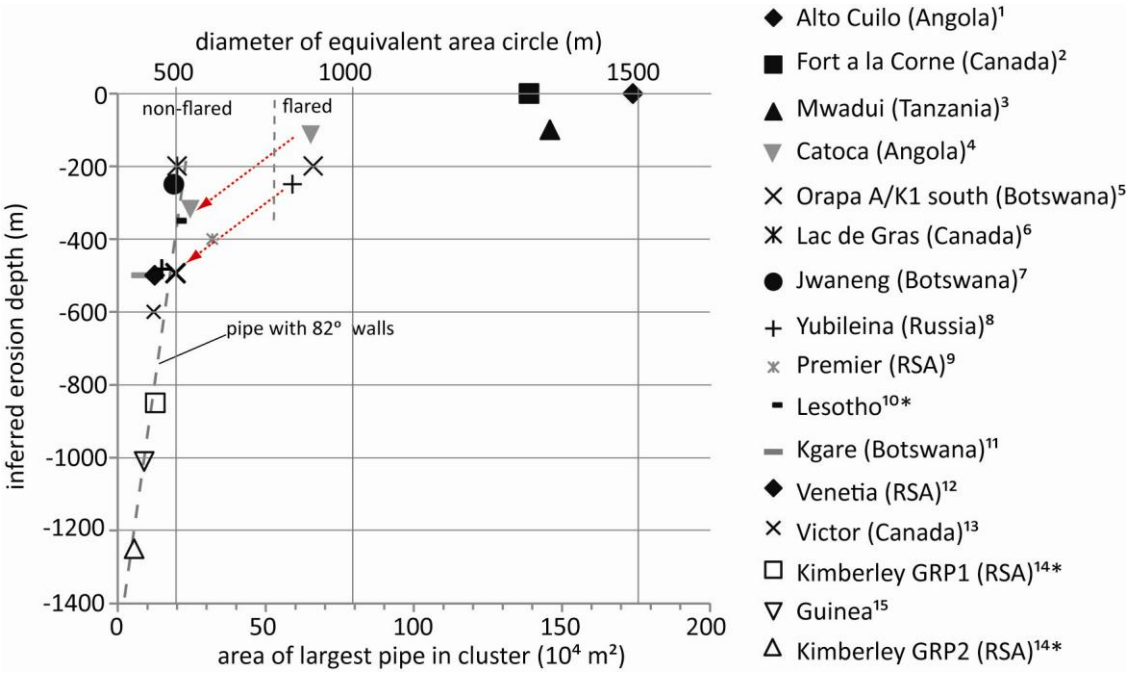
diameter of equivalent area circle (m)
500
1000
1500
0
-200
-400
-600
-800
-1000
-1200
-1400
non-flared
flared
pipe with 82° walls
inferred erosion depth (m)
0
50
100
150
200
area of largest pipe in cluster (10⁴ m²)
Alto Cuilo (Angola)[1]
Fort a la Corne (Canada)[2]
Mwadui (Tanzania)[3]
Catoca (Angola)[4]
Orapa A/K1 south (Botswana)[5]
Lac de Gras (Canada)[6]
Jwaneng (Botswana)[7]
Yubileina (Russia)[8]
Premier (RSA)[9]
Lesotho[10]*
Kgare (Botswana)[11]
Venetia (RSA)[12]
Victor (Canada)[13]
Kimberley GRP1 (RSA)[14]*
Guinea[15]
Kimberley GRP2 (RSA)[14]*

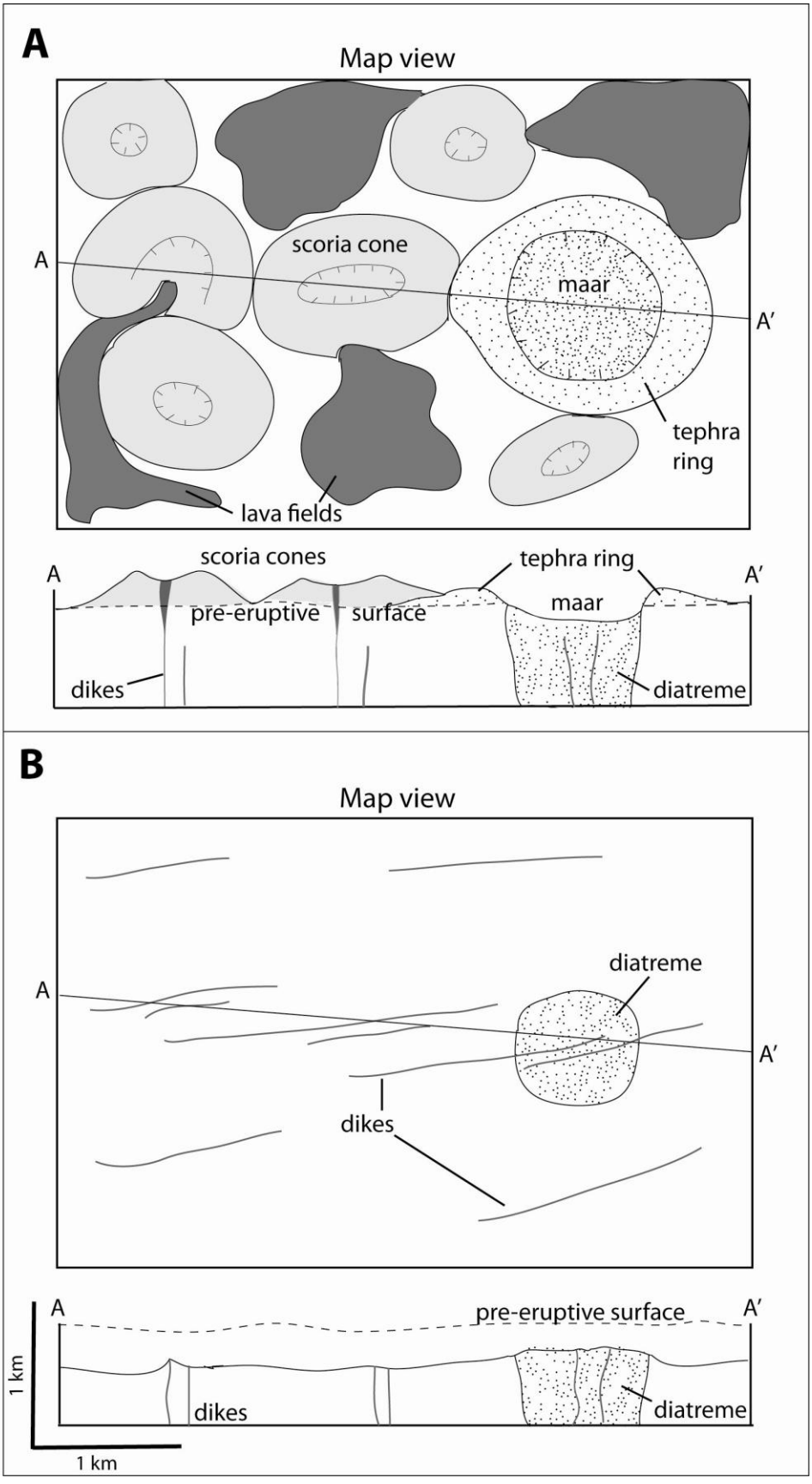
A
Map view
A
A′
scoria cone
maar
tephra
ring
lava fields
A
scoria cones
tephra ring
A′
maar
pre-eruptive
surface
dikes
diatreme
B
Map view
A
diatreme
A′
dikes
A
pre-eruptive surface
A′
1 km
dikes
diatreme
1 km